UC Berkeley
UC Berkeley Electronic Theses and Dissertations

Title
Silicon Nanowires for Chemical Sensing, pH Measurement and Ion Species Identificaiton in Solution

Permalink
https://escholarship.org/uc/item/0m94k81x

Author
Pace, Maria E.

Publication Date
2015

Peer reviewed|Thesis/dissertation

eScholarship.org Powered by the California Digital Library
University of California

Silicon Nanowires for Chemical Sensing, pH Measurement and Ion Species Identification in Solution

By

Maria E. Pace

A dissertation submitted in partial satisfaction of the

requirements for the degree of

Doctor of Philosophy

in

Applied Science and Technology

in the

GRADUATE DIVISION

of the

UNIVERSITY OF CALIFORNIA, BERKELEY

Committee in charge:

Professor Tarek I Zohdi, Co-Chair
Professor Albert P. Pisano, Co-Chair
Professor Liwei Lin
Professor Mohammad Mofrad

Fall 2015

Silicon Nanowires for Chemical Sensing, pH Measurement and Ion Species Identification in Solution

Copyright 2015

by

Maria E. Pace

Abstract

Silicon Nanowires for Chemical Sensing, pH Measurement and Ion Species Identification in Solution

by

Maria E. Pace

Doctor of Philosophy in Applied Science and Technology

University of California, Berkeley

Professor Tarek I. Zohdi, Co-Chair

Dean Albert P. Pisano, Co-Chair

In situ measurement of true pH would be useful in many applications. True pH is the negative log of the Hydrogen ion concentration, however, measurement of this is elusive in many practical applications due to the presence of interfering ions, such as sodium and potassium. Monitoring true pH in surgical procedures, for instance, would be very useful, however, interfering ions necessitate preprocessing of the blood and laboratory analysis making it not in situ, and not in real time. This work presents a measurement system capable of measuring true pH in the presence of interfering ions using nanowire sensors and electrospectroscopy. This system is also able to operate as a chemical sensor by discriminating between different ionic species in solution and can separately measure concentrations of other ionic species for leak detection and chemical identification. Nanowire sensors offer many advantages such as small size, low power, and inexpensive fabrication. These advantages allow real time, in situ monitoring in many applications.

In addition, silicon nanowires are integrated as a semiconductor pH sensor and species identification chip. Using electrospectroscopy, ions drift in the fluid at different times allowing the nanowire to make measurements of different species present in the fluid. To accomplish this, various modes of operation including "the time of flight" have been developed to maximize ion identification and species concentration measurement. The advantages of these sensors include high sensitivity at low concentrations, 80% sensitivity at 1e-6 M with ion species identification and measurement of true pH.

Depending on the species of interest, a particular mode of operation can be employed to achieve desirable results. Advantages of these modes of operation are isolation of hydrogen ions from other species including sodium to measure true pH in real time and a method for deconvolving the species both in temporal and spatial maps.

Additionally, a method for electrically cleaning the nanowires sensors and a method to re-zero the nanowires has been explored allowing more accurate measurement of the species and true pH.

A novel top down fabrication process has been developed which reduces the line edge roughness of the nanowire for more reproducible sensors, reduces dielectric pin hole

density for minimal sensor drift over time and reduces parasitic resistance for higher ion sensitivity. This novel fabrication process is truly CMOS compatible allowing more compatibility with other electronics. The SiNW is covered by thin film which protects SiNW from liquid penetration and can also work as ion sensitive film or functionalized surface. As a fabrication simplicity, the entire structure above can be built on a standard SOI (Silicon on Insulator) wafer. Experimental results have shown a linear relation between resistance change in the nanowire and pH in the fluid.

Dedicated to my lovely family:

Ana Maria Millan Jauregui, my son Nicolas Francisco Pace

and

Jack Pace and Teatha Van Schooten

for

their endless love, care and support

ACKNOWLEDGEMENTS

First, I would like to express my sincere gratitude to my advisor Dean Albert P. Pisano, for his encouragement, advice and academic and financial support. From him I have learned not just about science and engineering but about life and the world. He has shown me important skills to embrace even the biggest challenges in life. He has opened the doors for me to achieve my goals and he has given me the tools I need to be successful. He has always believed in me and that has given me the strength to make it through. I am forever grateful to him!

I would also like to thank Professor Tarek Zohdi for his understanding, advice, encouragement and support. I appreciate his guidance and motivation through challenging times and for facilitating the path to achieve my goals. I am also grateful to Professor Oscar Dubon for his academic and financial support and for his help to be admitted to AS&T so that I could complete my PhD. I am also grateful to Professor Mohammad Mofrad for his interest in my academic achievements and for his help and advice. I would also like to thank Professor Liwei Lin for inviting me into his group, for his advice and encouragement. I would also like to thank Professor Amy Herr for serving as the chair of my qualifying exam and for advising me on career opportunities.

I am very happy to have had the opportunity to work with Dr. Ono from Hitachi. His collaboration was a very positive learning experience.

A special thank you to Ariana Castro who was always available to listen, help me and encourage me through the challenges. I also would like to thank the staff at UC San Diego, Leah Kent, Kristi Ingles, Diane Lantz, Ann Kim and everyone else who supported me throughout this years.

To all the members of my group (BMAD, PRIME) for their support with my prelims and courses. To the nanolab staff and members for helping me with the process and the training.

To my friends Joanne Lo, Roseanne Warren, Levent Beker, Emmeline, Larry Lee, Alvaro Picon for all their support.

I would also like to thank everyone who along the way has supported me and has believed in me.

Finally to my mother Ana for her daily support, love, care, compassion and strength through every moment of every day. For teaching me perseverance, positive

attitude. To Jack for his unconditional support, love and care. To Teatha for her love and understanding, to my father who is watching me from up above and to my son Nicolas, my joy, my happiness and my love. My family which is the reason of my life, my strength and the fuel that drives me to succeed every day. I truly love you!

TABLE OF CONTENTS

DEDICATION i

ACKNOWLEDGEMENTS ii

TABLE OF CONTENTS v

LIST OF FIGURES x

LIST OF TABLES xvii

Chapter 1 Introduction 1

1.1 Motivation of Work 1

1.2 Background and Literature Review 2

1.2.1 Chemical Sensors 2

1.2.1.1 pH Measuring Devices 2

1.2.1.1.1 Paper Strips 2

1.2.1.1.2 Glass Electrode 3

1.2.1.1.3 ISFETS (Ion Sensitive Field Effect Transistor) 5

1.2.1.1.4 Silicon Nanowires as pH Sensors 5

1.2.1.1.5 Ion Mobility Spectrometer 6

1.2.1.1.6 Example of a Fluidic Dynamic Charge Sensor 7

1.2.2 Nanowire Sensors 9

1.2.3 Motion of Ions in a Fluid 10

1.2.4 Fabrication of Nanowires 12

1.2.4.1 Bottom up versus Top Down Fabrication 12

1.2.4.2 State of the Art Fabrication Process 13

1.3 Summary of the Thesis 14

Chapter 2 Physical System For Ionic Species Discrimination And Identification 16

2.1 Measurement System 16

2.1.1 Physical System 16

2.1.2 Methods and Modes of Operation 17

2.1.2.1 Operation 17

2.1.2.2 Time of Flight Mode 18

2.1.2.3 Ion Interference 21

2.1.2.4 Spatial and Temporal Maps of Ionic Species 22

2.1.2.5 Advantages of the Dynamic Measurement System 25
2.1.2.5.1 In Situ Cleaning of the Nanowire Sensor 25
2.1.2.5.2 Re-Zeroing the Nanowire Sensor 26
2.1.2.5.3 Driving the Nanowire for Resistance Measurement 28
2.1.2.5.3.1 Pulsing the Nanowire Sensor 28
2.1.2.5.3.2 Driving the Nanowire Sensor at the External Potential 29
2.1.2.5.3.3 High Frequency AC Nanowire Drive 31
2.1.2.5.3.4 Minimum Frequency AC 31
2.2 Other Modes of Operation 31
2.2.1 Variable Frequency 32
2.2.2 AC Modulation with DC Offset 33
2.3 Summary of Chapter 2 35
Chapter 3 Theory, Modeling and Simulation of Species Discrimination and Identification 36
3.1 Analytical Models 36
3.1.1 Ionic Concentration and Initial Conditions 36
3.1.1.1 Calculation of the Total Ionic Dose and Calculation of Areal Density Against the Electrode 37
3.1.1.2 The Gaussian Profile 38
3.1.2 Drift-Diffusion 39
3.1.3 Electric Field Calculation due to the Centered Ionic Charge Concentration in the Fluid 42
3.1.4 Resistance Depletion Analysis 44
3.1.5 Sensitivity Analysis 45
3.1.6 Off-Centered Concentration Profile Analysis 46
3.1.6.1 Off-Centered E-Field Analysis 46
3.1.6.2 Calculation of the Sensor Response with the vector Fields (off-Centered) 48
3.1.7 Dynamic Range 53
3.1.7.1 Retrograde Doping Profile 53
3.1.7.2 Scaling of the Nanowire Sensor 54
3.1.7.3 Complementary Nanowire with Opposing Doping Profiles 54
3.2 Modeling and Finite Element Analysis of Silicon Nanowire Sensors for Ionic Species Identification 55

Chapter 4 Fabrication of Silicon Nanowires for Ionic Species Discrimination and Identification **59**
4.1 Challenges in Existing State of the Art Processes 60
4.1.1 Line Edge Roughness 61
4.1.2 Sensor Drift Over Time 63
4.2 Novel Fabrication Improvements 63
4.2.1 Silicon Oxide Hard Mask 64
4.2.2 High Temperature Dielectric 66
4.2.3 Parasitic Resistance 66
4.2.4 Detailed Novel Fabrication Process 67
4.2.5 Fabrication Results of Silicon Nanostructures 69
4.3 Cell/System Fabrication 70
Chapter 5 Conclusions and Future Work **72**
References **74**

LIST OF FIGURES

Fig. 1.1	Schematic of pH meter	4
Fig. 1.2	Ion Mobility Spectrometer	6
Fig. 1.3	Results from DNA base pairs measurement using a FET	8
Fig. 1.4	Transistor used to detect small amount of charge dynamically.	8
Fig. 1.5	Example of top down fabrication process.	14
Fig. 2.1	Design of a cell with outer electrodes and one nanowire sensor	17
Fig. 2.2	A dynamic system with an external electric field in fluid	19
Fig. 2.3	Examples of (a) Glass electrode method of sensing pH and (b) a dynamic method for sensing pH	20
Fig. 2.4	Spatial and Temporal maps of the species as they cross the channel	24
Fig. 2.5	Results of Resistance versus time showing sensor drift over time	25
Fig. 2.6	Mechanism for improving sensor drift over time	26
Fig. 2.7	Electrically cleaning and calibrating the nanowire sensor in situ	27
Fig. 2.8	Pulsing the nanowire sensor to reduce disturbance of ions	29
Fig. 2.9	Driving the nanowire sensor at the correct potential	30
Fig. 2.10	Nanowire response due variable frequency	33
Fig. 2.11	Description of Mode of operation: AC modulation with DC offset	34
Fig. 3.1	Result of the concentration of H+ around the nanowire sensor	39
Fig. 3.2	Illustration of terminal velocity	41
Fig. 3.3	Result of resistance of the nanowire sensor versus pH	45
Fig. 3.4	Result of the sensitivity of the nanowire sensor versus pH	46
Fig. 3.5	Results of the two components of the electric field in the nanowire	48
Fig. 3.6	Illustration of the depletion region in the nanowire due to off-centered concentration of species	49
Fig. 3.7	Results of the response of the nanowire due to an off centered ion concentration at different doping concentrations	49
Fig. 3.8	Comparison of the result of the response by the silicon nanowire sensor when the x component of the electric field has been blocked	50
Fig. 3.9	Results of the x and z components of the electric field by the nanowire sensor for with pH = 5.	51
Fig. 3.10	Results of the comparison of the total electric field versus the electric	

	field with the x component for two species at pH = 5	51
Fig. 3.11	Illustration of the depletion region on the nanowire due to two species	52
Fig. 3.12	Results of the response by the nanowire for two species at pH =5 .	52
Fig. 3.13	Illustration of a retrograde doping profile nanowire sensor.	54
Fig. 3.14	Result of the ions migrating across the channel at various Δt	57
Fig. 4.1	Image of LER using SEM	62
Fig. 4.2	Image of LER for an array of silicon nanowires	62
Fig. 4.3	Schematic diagram of the novel fabrication process	68
Fig. 4.4	Fabricated silicon nanowire arrays	69
Fig. 4.5	Result of real-time pH measurement by silicon nanowire sensor for pH=4, 7 and 10	70
Fig. 4.6	Schematic diagram of the outer electrodes fabrication process.	71

LIST OF TABLES

Table 1.1	Mobilities of ion species in water	10
Table 1.2	Diffusivities of ionic species in water	11
Table 3.1	Results comparison between modeling and analytical	58

CHAPTER 1. INTRODUCTION

1.1. Motivation of Work

This work presents, for the first time, a new technique to identify and quantify ionic species in solution. This novel technique uses electrodes on opposite ends of a cell to impose electric fields to force ion migration via a drift-diffusion mechanism. Nanowire charge sensors within the cell dynamically detect the presence of the mobile ionic charge in solution. Several distinct modes of operation are disclosed to separately identify and quantify the ions present.

The device consist of one or more silicon p-type nanowires placed in a fluidic channel surrounded by tall walls (outer electrodes). A potential difference is placed in between these two walls or outer electrodes that generates an electric field. The ions in the fluid respond to this electric field by migrating from one electrode to the other crossing the fluidic channel and disassociating themselves as they travel since each specie has a different mobility. When the ions are in the presence of the silicon nanowire, a change in electrical resistance can be measured at the nanowire and this electrical resistance corresponds to a particular pH or concentration.

Several pH devices are presently in used in industry to measure pH. Examples of these devices are the glass electrode, paper strips, ion sensitive field effect transistor, silicon nanowires, etc. However, these devices present several challenges, for instance, paper strips may lack resolution to detect small concentrations, ISFETS and glass electrodes are slow devices because they rely on diffusion of the species in the fluid to reach the device, as a result, they require several seconds before a measurement can be made, another challenge is selectivity of the species. Often times, there is interference of ions such as sodium which lead to the wrong measurement. Nevertheless, the system of semiconductor nanowires presented in this work offers the ability to separate the species

in solution and dynamically measure their concentration allowing for fast response (in microsecond regime), high sensitivity and high selectivity.

1.2. Background and Literature Review

1.2.1 Chemical Sensors

1.2.1.1 pH Measuring Devices

Many chemical processes such as pharmaceutical, medical, food production, pollution control and laboratory instrumentation require the measurement of pH in a solution. pH is defined as the negative log of the hydrogen ion activity in a solution. A common example, a neutral pH of 7, corresponds to an active hydrogen ion (H+) concentration of 10^{-7} mol/L. pH generally describes how acidic or alkaline a solution is. In a commonly accepted scale, pH ranges from 0 to 14. A solution is said to be acidic if it has pH of less than 7 or alkaline or basic if it has a pH higher than 7, with pH=7 being neutral. Water under standard temperature and pressure is commonly referred to as neutral (pH=7) though it is rare that water is maintained in a purely neutral state due to absorbed ions from the surrounding air. This scale does not represent all possible conditions. Some acids have pH lower than zero and some alkaline solutions have pH higher than 14 but these solutions are typically very reactive and not commonly encountered. The measurement of true pH (hydrogen ion activity) is of particular interest in the medical field to monitor pH during a surgical procedure but current methods require ex-situ processing of the blood or fluid and therefore cannot be done in real time as the surgery is taking place. True pH is challenging to measure in blood because of high concentrations of interfering ions such as sodium, potassium and chlorine. Most real-time sensors for pH seek to measure specifically hydrogen, but interfering ions contaminate the measurement and give erroneous readings [1].

1.2.1.1.1 Paper Strips

The most common method in use for pH sensing is pH indicating paper. The chemically treated paper changes color in response to a chemical reaction with the fluid under test. Resultant color from the paper strip is compared, either by eye or using a colorimeter, to a reference scale. Paper strips often suffer from poor dynamic range because of the difficulty in resolving small color differences between two samples that are close in pH value. Paper that measures smaller pH range is also available but the limitation is that the color is often times difficult to interpret with accuracy. For improved

dynamic range using paper strips, multiple strips covering different pH ranges are necessary for sensing over an arbitrary range [2].

1.2.1.1.2 Glass Electrode

Developed around 1960, glass is synthesized with the intent to specifically bind only Hydrogen ions to its surface, excluding other positive ions present in the solution like sodium. However, the sensitivity to hydrogen (H+) is not absolute, so there exists ion interference from other positive charges in the solution, which leads to a measurement that is not absolute in pH. Interfering ions that bind to the surface contaminate the true pH measurement. The glass used in a glass electrode for pH measurement typically has an OH- terminated surface (referred to as the site binding model), leading to problems with interference due to, for example, some sodium (Na+) ions adhering at the surface in a salt solution. If the pH is high (eg: 7+) and the salt concentration is high (eg: 1 millimolar) which is typical in seawater or blood, then even a small loss in specificity to hydrogen (H+) leads to a large error in true pH measurement because the interfering ion (Sodium) is several orders of magnitude higher in concentration than the hydrogen ions (H+) that the measurement seeks to quantify [3].

This pH meter is composed of a glass electrode and a reference electrode. Since electrical potential at any point is arbitrary, it must be referenced to another potential for any meaningful comparison. For that reason, a reference electrode must be used to provide a consistent potential reference. Then, a potential difference is measured with a sensitive voltmeter to provide an indication of pH. The glass electrode contains a buffer solution of known pH in contact with a known metal. When a separate electrode is placed in contact with the unknown solution, the hydrogen ions in the unknown solution bind to the surface of the glass electrode and a voltage difference is generated. This voltage is subtracted from the voltage known for the buffer solution and the resultant voltage difference is proportional to a specific ion concentration or surface charge, and therefore can be correlated to the solution's pH. The greater the potential difference a greater difference in hydrogen ion activity (and therefore "pH") in the unknown solution compared to the reference buffer solution [4].

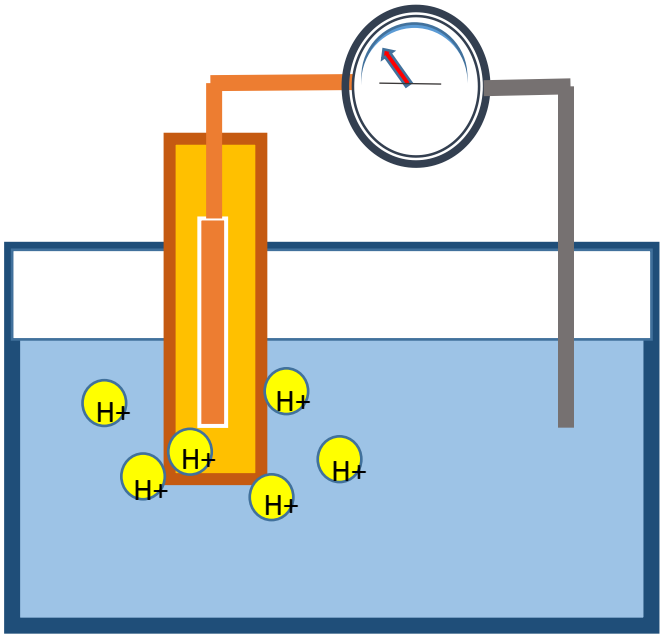

Figure 1.1 is an image of a pH meter. It has a glass electrode, shown in orange, made out of a conducting material such as silver/silver chloride immersed in a fluid of known pH, typically neutral (pH=7) and a reference electrode also made out of a conducting material. When the pH meter is submerged in the blue unknown solution, the hydrogen ions of the blue solution begin to diffuse toward the glass electrode and replace some of the metal ions inside it. At the same time, some of these metal ions also make it into the unknown blue solution and since the two solutions have different pH, then there is different amounts of hydrogen ion activity created on both sides of the glass electrode. The difference in hydrogen ion activity means that there is also a difference in potential between the two sides of the glass electrode. This difference in potential generates a voltage difference between the glass electrode and the reference electrode and this voltage is recorded by the meter in between them.

1.2.1.1.3 ISFETS (Ion Sensitive Field Effect Transistor)

ISFETs resemble a traditional Complementary Metal-Oxide Semiconductor (CMOS) transistor, except that the gate conductor has been removed and replaced with an ionic fluid under test, and the gate dielectric is designed to bind hydrogen ions (H+) as in the glass electrode. The electric field effect in the channel (which modulates the current in the transistor) is now caused by the bound charge from the fluid. The electrochemical effect is very much like the glass electrode, with the principal difference that sensing of charge bound to the glass surface is performed by a field effect transistor rather than a simple potential difference measurement. This provides built-in gain very near the charge/glass interface, and therefore a more sensitive, less noisy measurement of the bound charge is obtained. A reference electrode is also required in an ISFET system in order to make a meaningful measurement.

The terminated OH surface binds charge (+ or -) and is therefore capable of either accepting or rejecting a proton. Like the glass electrode, the ISFET suffers from the same lack of specificity since reactions with ions other than hydrogen (H+) contaminate the reading of true pH [5,6].

1.2.1.1.4 Silicon Nanowires as pH Sensors

The Nanowire sensor operates via a semiconductor charge depletion mechanism. The nanowire is covered by a very thin dielectric (glass) that binds hydrogen ions from the fluid under test. The nanowire is doped, in this example p-type, such that the majority carriers in the semiconductor are positive holes. When the positive charges bind to the surface, an electric field directed toward the nanowire results. This electric field causes positive majority carriers within the semiconductor to be electrostatically repelled from the periphery, toward the core of the nanowire, forming a region depleted of mobile charge carriers. Since the cross-sectional area of the nanowire now available for conduction has decreased to the central core, the electrical resistance along its length increases. Conversely, a decrease in the positive ion concentration in solution, or increase in negative ion concentration will cause an accumulation of positive charge carriers in the semiconductor, which will decrease electrical resistance of the nanowire. This electrical resistance is the sensed quantity that is used for pH measurement. A complementary

device is also possible, where the majority carriers in the semiconductor are electrons (n-type semiconductor), and the electrical response is opposite. The present work uses only p-doped nanowires [7,8].

1.2.1.1.5 Ion Mobility Spectrometer

Ion Mobility Spectrometers are devices that separate or distinguish ions in solution based on the value of each ions' mobility in that solution, most usually a gas-phase solution. Mobility is defined as the proportionality constant between ion drift velocity and the electric field driving the drift.

$$(V=\mu E)$$

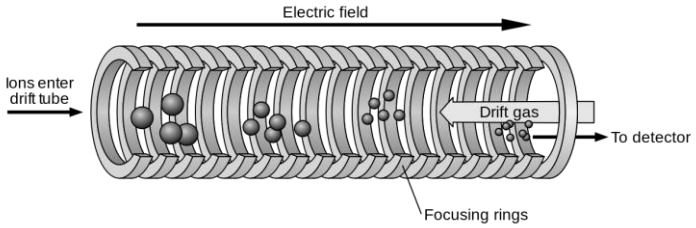

Figure 1.2 "Ion Mobility Spectrometry Diagram" [9]. The ions enter the tube through one end. Each ionic species has a different mobility. At the opposite end of the tube a drift gas enters in opposite direction as the ions. The drift gas causes the ions to slow down and separate into groups of the same species due to their difference in mobilities. Ions with higher mobility will travel faster than ions with slower mobility. At the end of the tube, a detector senses the species. Depending on the time the ion takes to reach the detector and the distance traveled, a mobility can be observed and this mobility (a unique property) corresponds to a particular species.

Ion mobility spectrometers (IMS) have many advantages [10]:

a). IMS can operate at atmospheric pressure without the need to pump vacuum,

b). Vapor-phase molecules are easily ionized,

c) Gas-phase ion separation which leads to ion identification

d) The response time is in the range of milliseconds.

e). Relative to other analytical instruments they are simple, have high selectivity and sensitivity. Sensitivity can be quite high, often reported in the range of part-per-billion.

Typically the molecules in the gas are not initially ionized, and therefore must first be ionized by adding or removing electrons. Ionization of the gas molecules is done by different methods such as corona discharge, ATM pressure photoionization (APPI), electrospray ionization (ESI) or radioactive source ionization with Ni or americium (a common method used in household smoke detectors).

Selectivity depends on various factors such as the method used to ionize the source and the amount of ion separation that can be achieved before it reaches the detector. Because of incomplete ionization, calibration is usually necessary for quantification of concentrations of ions.

Measuring very small charges suspended in a liquid is more challenging because it is more difficult to separate the species than in gas form due to the mobility difference between the different mediums due to viscosity [10].

1.2.1.1.6 Example of a Fluidic Dynamic Charge Sensor

Until now, nanowire pH sensors measure charge amounts statically, that is waiting a period of time before the charge of interest binds on a surface and then measuring the steady state concentration of these charges. The pH sensors presented thus far are based on a surface reaction. The question arises, is it possible to measure small concentrations of charge dynamically, as the charge flows past a nanosensor, possibly at some distance, without being bound to a surface? The following device is an example of a dynamic charge sensor where the charge is measured as it passes through the sensor in real time.

Measurement of very tiny amounts of charge is possible in a liquid, as demonstrated by EAGLE research for direct electrical readout of DNA (Deoxyribonucleic acid) base pairs. DNA, present in the cells of all living things, is a long string made of billions of base pairs, separated by about a nanometer. Each base pair has a very small amount of charge, and that charge is distinct depending on the specific

base pair (either A, T, C or G). EAGLE is able to read the exceedingly small charge pattern of a single strand of DNA dynamically in a fluid as the strand passes a charge sensor at some distance from the surface (likely very close proximity).
Using a small field effect transistor as a charge sensor, positioned in a small pore the DNA charge was measured. The transistor is able to detect the charge signature of each base pair as the single stranded DNA passes by the transistor's gate region as shown in Figure 1.3

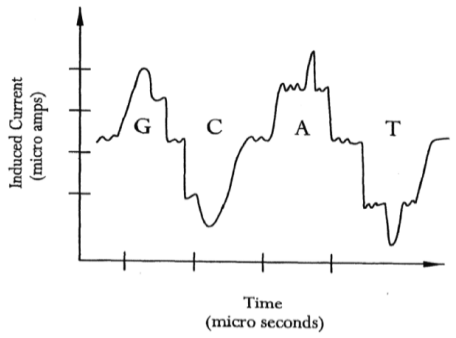

Figure 1.3 shows the experimental results from measuring tiny amounts of DNA. Each base pair can be distinguished [11].

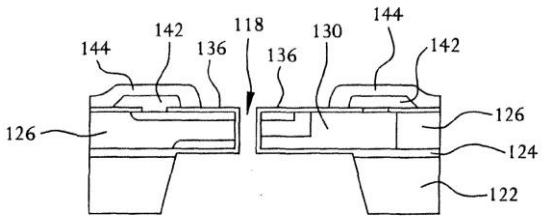

Figure 1.4 EAGLE etched a pore in a silicon on insulator (SOI) device layer, and a transistor is built vertically. Fluid is forced through the small pore, thus forcing suspended DNA to pass in very close proximity to the channel region of the vertical transistor. For every base pair of single strand DNA, there is very small associated charge and that charge creates a unique electrical response or signature as it goes through the pore and past the transistor [11].

The implication of this work on the present work is that a minute amount of charge can be detected from the solution and the transistor is sensitive enough that it can distinguish between the four distinct DNA bases, A, T, C, and G, with each base pair being separated by only a few nanometers. Thus, it is possible to measure tinny amounts of charge dynamically, without being bound to the surface.

1.2.2 Nanowire Sensors

A nanowire is a pseudo 1-dimensional structure. It has effectively infinite length (in relation to the other dimensions) and has nanometer-scale dimensions in the width and height directions. Nanowires have certain interesting properties owing to their exceedingly small scale in two dimensions

1). In some cases, quantum mechanical effects can be observed; for example, the electrons in a nanowire are quantum confined laterally and as a result occupy discrete energy levels differently from the continuum energy levels or bands seen in bulk or 3-D materials. This confinement can lead to quantization of density of states (DOS) in a semiconductor nanowire. The present work does not directly make use of quantum effects in nanowires [12].

2). In this work, nanowires are used primarily because of advantageous surface to volume ratio which leads to higher sensitivity to surrounding charge. When scaling the nanowire to smaller dimensions, the surface to volume ratio is increased. Because of the high Surface/Volume ratio, a surrounding surface charge density from adhered hydrogen ions (H+) will produce a larger electric field in the interior volume of the nanowire, and therefore a larger percentage change in resistance in the nanowire due to carrier depletion. This operation is described more in detail later [13].

3). Another aspect of the nanowire useful in this work is that the nanowire can spatially pinpoint, in at least one direction, the electric field due to surrounding charge, and can therefore be useful in the very small electrochemical cell necessary in this measurement system. This is advantageous in sensing distinct species and determining the concentration of the species present in the fluid at a very precise location in space. Additionally, multiple nanowires can be packed

in a small area to produce spatial maps.

Until now, the nanowire sensors relied on the diffusion of the ions to the surface of the nanowire and binding of the fluid ionic charge to the surface. The charges diffuse in the fluid and adhere to the surface of the nanowire until an equilibrium is reached, much like a glass electrode, resulting in a change in resistance in the nanowire that can be measured. Park states that the nanowire response time for charges to diffuse in the fluid to the surface of the nanowire is measured at approximately 6 seconds before steady state is achieved [14].

1.2.3 Motion of Ions in a Fluid

Ions in a fluid move separately from the fluid flow primarily by two mechanisms: drift and diffusion.

Drift is the velocity of the ions in the fluid in response to an electric field. Each species of ions has a corresponding mobility which is the ratio of the drift velocity to an applied electric field. See Table 1.1. Equation (1) describes drift velocity where V is the velocity of an ionic specie in the fluid, μ is the mobility of the species and E is the electric field.

$$V = \mu E \qquad (1)$$

(The drag force opposes the oncoming direction of the velocity of the species)

Ion Species	**Mobility** (μ^2/Vs)
Hydrogen (H+)	360,000
Hydroxide (OH-)	205,000
Chlorine (Cl-)	79,000
Potassium (K+)	76,000
Sodium (Na+)	52,000

Table 1.1. Mobilities of ion species in water [16]. The mobility of Hydrogen is quoted as the mobility of H+, but the mechanism is actually more complicated, involving Hydronium (H_3O+). The proton moves in the fluid by protonating H_2O and hopping from molecule to molecule, creating H_3O+ as an intermediate species. This is known as the Grotthuss mechanism [17].

Drift, as a mechanism of ion migration, assumes that the ions have, for all purposes, reached terminal velocity. This assumption is discussed and verified in Chapter 3.

Diffusion is caused by random thermal motion of the ions, which over time leads to a spreading of the species concentration toward a more uniform distribution. The flow of ions under diffusive action is always from a region of higher concentration to a region of lower concentration. At any finite non-zero absolute temperature, Diffusion is always occurring and is a function of the temperature for a given ion [18].

$$D = \frac{KT}{q}\mu \qquad (2)$$

Equation (2) describes diffusion. D is the diffusion coefficient or diffusivity, K is the Boltzmann constant, T is temperature, q is the charge of an electron and μ is the ion mobility. This equation is known as the Einstein relation and relates diffusivity to mobility and therefore relates diffusion and drift. This simple relationship is important for a mobility spectrometer because it implies that drift and diffusion are not independent mechanisms, and for sensor purposes, cannot be controlled independently, except by changing temperature. In mobility measurement, diffusion is generally a parasitic effect that should ideally be minimized, but this is only possible by reducing the temperature of the fluid. Generally, this is impractical, and can only be theoretically reduced to approximately 273K for water-based solutions, which would only offer slight improvement over room-temperature measurements (293K).

The following is a table of Diffusion coefficient for several ionic species of interest at room temperature (300 K) [19]

Ion Species	**Diffusivity** (μ^2/s)
Hydrogen (H+)	$9.36*10^3$
Hydroxide (OH-)	$5.33*10^3$
Chlorine (Cl-)	$2.054*10^3$
Potassium (K+)	$1.976*10^3$
Sodium (Na+)	$1.352*10^3$

Table 1.2. Diffusivities of various ionic species in water

1.2.4 Fabrication of Nanowires

Due to their physical properties, nanowires have been the subject of intense research in many fields including medicine, biology, physics, and microelectronics. As a result, advances in nanowire fabrication techniques have evolved over the past few decades leading to primarily two different fabrication methods: one is a top down approach and the other one is a bottom up approach.

1.2.4.1 Bottom Up versus Top Down Fabrication

In the bottom up fabrication process, nanowires are formed through atom-by-atom growth, synthesis, or deposition wherein process conditions and starting seed structure dictate the final structures. This method can produce very small atomic-scale nanowires such as single-wall carbon nanotubes. The principal drawback of this fabrication method is the difficulty of integration with microelectronic components and external circuitry, because it is often difficult to control the location and exact dimension of the resulting nanowire.

A Top down fabrication process consists of selective removal of layered material from the nanowires, similar to a thin-film semiconductor fabrication process. The main advantage of this method is the use of existing mature semiconductor fabrication tooling and methods. The resulting nanowires are generally larger, often being limited by the process used to pattern the planar dimensions of the structure. While many pattern generation techniques exist for the top-down approach, the patterning method used in this work is nanolithography using direct-write electron beam lithography with a photoresist mask. Pattern transfer is accomplished by plasma etching techniques to fabricate the nanowires in semiconductor materials as discussed in chapter 4. The reliably achievable lithographic dimensions are tens of nanometers. A second limitation of the electron beam patterned nanowires is the time required to generate the pattern, as each individual nanowire must be written serially in time. The nanowires themselves are not particularly time consuming to write with the electron beam but the necessary interfacing structures such as bond pads and connecting wires (large features) take a significant amount of time to write which makes the process expensive for writing many nanowire systems. An

optical/e-beam hybrid technique has been employed by other researchers in the field, and that technique is improved in the present work.

While the present work uses a top-down approach for fabricating nanowires, the techniques and operation of the sensing system are amenable to using bottom-up fabricated nanowires, once the methods for making them are sufficiently mature for consistent and reliable devices. The fabrication process will be different, but the principles of operation remain the same [20,21,22, 23, 24].

1.2.4.2 State of the Art Fabrication Process

A state of the art fabrication process using a top down method is described here. An improved process is described in chapter 4 which overcomes some of the limitations of the process presented in this section.

A silicon-on-insulator (SOI) wafer is used with a device layer thickness of approximately 200 nanometer provided by the manufacturer. To reliably thin down this layer, thermal silicon dioxide growth is used as a sacrificial method since the growth process consumes about 44% of underlying silicon for a given growth thickness. This silicon oxide is then removed by wet chemical etching, resulting in a highly predictable thinner silicon device layer. This process can be repeated multiple times for more accurate "trimming" of the device layer thickness. Next, electron beam lithography is used to open up a very narrow trench in e-beam photoresist. This narrow trench will eventually form the nanowire sensor. A layer of chromium is deposited followed by liftoff of the chromium lying on top of resist. The chromium remains only in the nanowire trench feature. Optical lithography is then used in a similar way to form the pads and leads (large features) as negative-tone images in standard optical photoresist, and Chromium is again deposited followed by liftoff. The chromium remains where the pads and leads are formed. The nanowire region is protected by optical resist (except for some small overlap to ensure an electrically contiguous structure) during the second chromium deposition. This hybrid two-step imaging process results in a composite structure where larger microscopic features have been defined (rapidly) by optical lithography and nanoscopic features have been defined by (more tedious) e-beam lithography. Next, the silicon is etched in a chlorine plasma while the chromium serves as a hard mask in order to form the device. Following the silicon etch, the chromium is removed by a wet etch process, leaving a nanowire and large leads and bond pads entirely in a thin device layer of silicon. A thin blanket layer of silicon nitride is deposited by plasma enhanced chemical vapor deposition over the nanowire and then etched away in the bondpad/contact region using a conventional semiconductor process. Finally, a metal deposition and liftoff process is used to form the contacts suitable for interface to electronics for testing [25, 26].

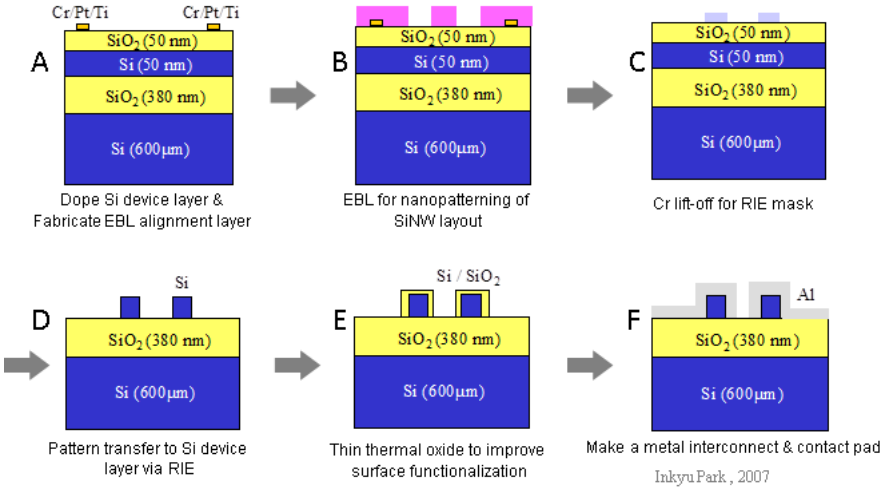

Figure 1.5 describes Park's fabrication process [25]. This is a top down fabrication process that uses double chromium deposition and lift off to form the small and large features.

Some of the problems and challenges with this method are

1). Very small pinholes in the nitride dielectric passivation, leading to electrical leakage between the fluid and the nanowire

2). Line edge roughness (LER) on the nanowire. Instead of the nanowire having straight, smooth sidewalls, the surfaces are rough and wavy. This also results in the nanowire having inconsistent cross-section along its length.

3). A sensor output drift over time.

These issues are addressed in Chapter 4 in an improved process, and the sensor output drift is additionally addressed by novel electrical driving methods, covered in chapter 2.

1.3. Summary of the Thesis

This work presents a novel technique for measuring true pH in situ, in real time, without previous processing of the liquid and a novel method for analyzing the fluid by measuring its various ionic species. Chapter 2 introduces a novel physical system using silicon nanowires and outer electrodes to achieve measurement of true pH and ion identification. This chapter also includes advantages of the system such as in situ

electrical cleaning of the nanowire and a method to re-zero the sensor to minimize sensor drift, a description of a novel technique to control the ionic species using a potential difference between the outer electrodes and other modes of operation. Chapter 3 analyzes one mode of operation in detail, the time of flight mode, with detailed physical models and finite element analysis. The details of dynamic time constants is also discussed. Chapter 4 explains the fabrication challenges in the state of the art and introduces a new fabrication process with improved ideas to make the system more sensitive. A two-substrate bonded process is introduced as a method for forming tall channel walls integrated with nanowire sensors to form the complete drift-diffusion dynamic sensor. Chapter 5 is the conclusions and future work. Ideas that can help improve this sensor and extend this work are presented here.

CHAPTER 2. PHYSICAL SYSTEM FOR IONIC SPECIES DISCRIMINATION AND IDENTIFICATION

This chapter describes the physical system used to separately identify ionic species and quantify the concentration of each ionic species present in the fluid.

2.1. Measurement System

2.1.1 Physical System

Identifying and quantifying ions in liquid is challenging primarily due to interference of ions and the need for sensitivity of the sensor. However, this works presents, for the first time, a novel physical system that overcomes these challenges and achieves a rapid response. Figure 2.1 represents a cross-sectional image of this unique system.

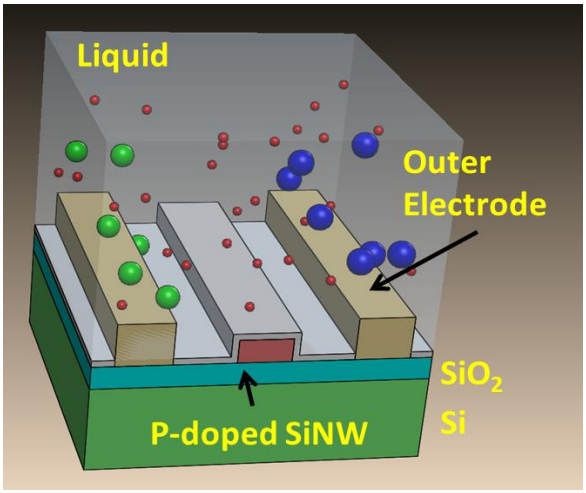

Figure 2.1 A dynamic system with a single nanowire sensor in between two outer electrodes submerged in a fluid with various ionic species.

The outer electrodes are located at opposite sides of a fluid channel. These outer electrodes are tall conducting walls. In the center of the figure, a silicon nanowire sensor is located over silicon oxide layer on the substrate. An ionic liquid is present in the cell and can be flowing or stationary. Fabrication of the system is described more in detail in chapter 4.

2.1.2 Methods and Modes of Operation:

2.1.2.1 Operation

In order to operate this device, numerous modes of operation have been developed. Nevertheless, the preferred mode of operation is referred to here as “the time of flight mode”. The reason why the time of flight mode of operation is preferred is because of its simplicity to achieve discrimination of ionic species which also achieves a measurement of the true pH along with measurement of other ionic species present in the fluid. Each mode of operation has advantages and disadvantages depending on the fluid under test, the desired species or quantity to be measured and other environmental factors. Time of flight mode is described first in section 2.1.2.2. Other modes of operation are described later in section 2.2.

2.1.2.2 Time of Flight Mode

Historically, measurement of pH has relied mostly on the glass electrode method. Nanowires have been employed as the sensing element recently, but the surface charge mechanism is similar to the glass electrode method used since about 1960 [3, 4].

The surface charge method requires that charged ions diffuse through the fluid to the glass surface and attach or bond. An equilibrium surface charge is reached after some time, which may be considerable-- on the order of at least 6 seconds [8]. In the case where a nanowire is used to sense the bound charge, a change in potential causes a change in electrical resistance proportional to the fluid pH. This change in resistance comes from the depletion region in the nanowire. One disadvantage of this method is that diffusion in the fluid is not rapid, making the time for the overall sensor response slow. It is important to note that this is not limited by the charge sensor (nanowire) itself, but by the diffusion process in the fluid. Another disadvantage is that it is not fully specific to one ion (H+) which leads to a false reading of the true pH (Hydrogen ion activity). Again, this specificity problem is not caused by the charge sensor, but by the limitation of the available glass and its ion specificity.

In this work, for the first time, dynamic true pH measurement is studied by a new method that combines some of the ideas presented in Chapter 1.

As shown in Figure 2.2 an external electric field is applied between the outer electrodes to force ion drift. Using this external electric field, ions of different species separate initially into two groups. The positive ions move to one side of the cell, collimating against the negative electrode and the negative ions move to the opposite side collimating at the positive electrode and depleting the fluid from any mobile charge. When the electric field is reversed, the ions drift from one side toward the other side

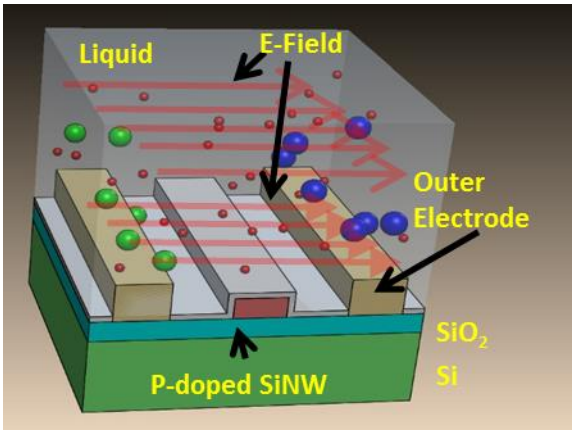

Figure 2.2 describes the dynamic system. The arrows represent the external electric field. The ions move in response to the electric field.

Since each species of ion has a corresponding distinct mobility in the fluid, the ions will move at different speeds separating each species from one another into groups of ions. These ionic species have different mobilities so they traverse the cell at different average speeds [16]. The ion concentrations are also subject to diffusion, so each species will form a gaussian profile moving across the channel. The average velocity of the gaussian peak will correspond to the mobility of the species, with the spreading of the gaussian profile with time due to each species diffusion.

An array of nanowires sensors are fabricated to sense the electric field due to the moving ions. As ionic species travel across the channel, the nanowires are able to detect the real-time positions of the charge. The sensing mechanism of the nanowire as a charge sensor is electrostatically similar to that in the bound surface charge method-- the nanowire senses the surrounding charge and therefore a depletion region is formed in the nanowire which leads to a change in resistance. However, the ions are not bound at the surface, and are, in general, much further away from the surface of the nanowire. The E-field due to each unit charge is therefore much lower, since the electric field is given by Equation (3) where E is the electric field, k is the Coulomb's constant, q is the magnitude of the charge and r is the distance between the charges.

$$E = \frac{kq}{r^2} \qquad (3)$$

As a species crosses the nanowire, the charges being sensed are distributed roughly vertically above the nanowire senor, spread horizontally in a diffused Gaussian profile.

The charge being sensed by the dynamic nanowire sensor system is changing rapidly when compared to the surface charge binding method described previously. See Figure 2.3 A Gaussian profile may pass the nanowire sensor in a few microseconds, whereas diffusion times in the surface charge binding method requires several seconds.

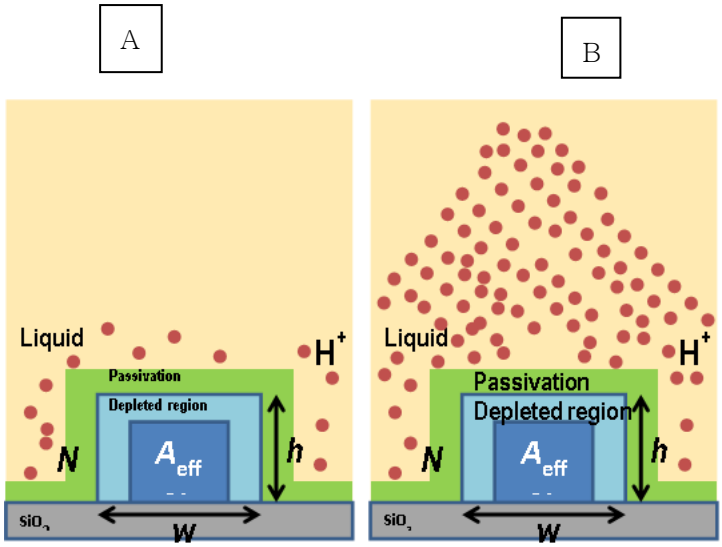

Figure 2.3 A) describes a nanowire sensor that relies on diffusion and surface binding of ions to adhere at the surface. (aka: Glass electrode) B) Shows a dynamic system with a Gaussian profile around the nanowire sensor as the ions travel in response to the external electric field.

A potential disadvantage of this dynamic method is that sensitivity is not as high per unit charge, but it must be remembered that even though the charge is at a larger distance from the sensor, and the electric field is inversely proportional to the square of the distance, there are potentially many more charges participating in the measurement. In the case of surface binding, the surface binds an equilibrium charge density depending on the pH. For the dynamic sensor, most all charges of each species contained in the volume of the cell will participate in forming the sensed electric field. Therefore, sensitivity depends on the volume of the cell because the cell collects all charge from the entire volume, and compacts it into a smaller space using the external electrodes, the total

charge being measured, at peak, from the dynamic system is approximately all of the charge in the cell. For the surface charge glass electrode, only a small fraction of the available ions are sampled and measured, based on an equilibrium surface condition. Clearly, the design details of the dynamic system are important: A cell too large allows too much diffusion between the concentration of the collected charge and its measurement. A cell too small provides insufficient charge for measurement.

In the time of flight mode, there are conflicting design criteria for optimal measurement. On the one hand, it is desirable to measure the species soon after the ions leave the wall, so that diffusion is minimal. On the other hand, it is desirable to wait some time/distance to make the measurement so that faster ions can become more separated from slower ones. Thus, in order to improve sensing of the ionic species, placement of the nanowire sensors in the channel is a critical part of the design. Depending on the species of interest that need to be measured, the location of the nanowire sensor can be chosen to maximize the sensing. In an extreme example of ion interference, a negative ion profile traveling from the right to the left will, at some point, overlap a positive ion profile traveling from left to right. If their concentrations are the same, the sensor response will be exactly zero since the charges are opposite sign. The use of these outer electrodes and nanowires together constitutes a system in which differentiation and ion velocities are used as a way to gather or move ions of different charge to mobility ratios.

2.1.2.3 Ion Interference

Ion interference is one of the main challenges in the type of sensor described in this work because it obscure the reading leading to an erroneous measurement. Ion interference can occur two different ways.

One interference mechanism is when the fluid contains two or more positive species such as sodium and hydrogen. In the case of the system presented in this work, all positive ions initially collimate against one electrode and begin to drift and diffuse across the channel as the electric field has switched. Separation of these species occurs based on ion mobility and true pH and the concentration of each species can be determined by

measuring the different Gaussian peaks that cross the nanowire sensor at various times. If the species have not spatially separated sufficiently when they arrive at the nanowire, then the nanowire sensor will measure the total combined charge leading to a false reading. This type of interference is more predominant in liquids where the concentration of sodium is significantly greater than the concentration of hydrogen as is the case of blood or salt water. (Also, when trying to discriminate ions of numerically similar mobility values, spatial separation is challenging.) The Gaussian tails of the sodium peak may extend into the weaker hydrogen peak, overwhelming it, and obscuring an accurate determination of the Hydrogen concentration. This interference is analogous to the specificity problem in a surface charge glass electrode device for pH measurement. The surface is designed to selectively attract hydrogen ions specifically, however, sodium ions interfere with the hydrogen ions by non-selective binding. Sodium ions binding to the glass where only hydrogen are expected artificially alters the pH measurement. But the physical mechanisms of interference are completely different, and therefore can be optimized for different solutions or measurement purposes.

The second interference mechanism occurs when ion interference is present is when two species, one positive such as hydrogen and one negative such as hydroxide, arrive at the nanowire simultaneously but from opposite directions. Therefore, if the concentration of both species is about the same, then the positive charges cancel the negative charges and the nanowire sensor reads essentially zero as if no charges have traveled across. To minimize these two interferences, placement of the nanowire sensor in the channel is critical. Depending on the species of interest, the system can be designed accordingly. Multiple nanowires can be placed and measured for more general systems.

2.1.2.4 Spatial and Temporal Maps of Ionic Species

As mentioned earlier, designing the cell is very important in order to sense the species of interest. To understand how the design can be most optimum, both temporal and spatial maps of the species concentrations can be shown and measured with sufficient spatial and temporal resolution. For example, the system with 2 nanowires, each close to the walls contains two nanowires located in the vicinity of the outer electrodes. Soon after the ions have collimated against the outer electrodes and the electric field has

switched, these two nanowires can capture the concentration of each species with minimal diffusion. The further distance the species travel, diffusion becomes more dominant and the Gaussian profile spreads spatially. However, an important advantage of this dynamic measurement system is that nanowires are very small in width, thus, an array of nanowire sensors can be easily fabricated across the channel. The advantage of this is that now spatial and temporal maps of the ionic species can be analyzed as in Figure 2.4. Therefore, data can be deconvolved and a more accurate determination of species and their concentrations can be achieved. A larger data set also provides for higher noise immunity.

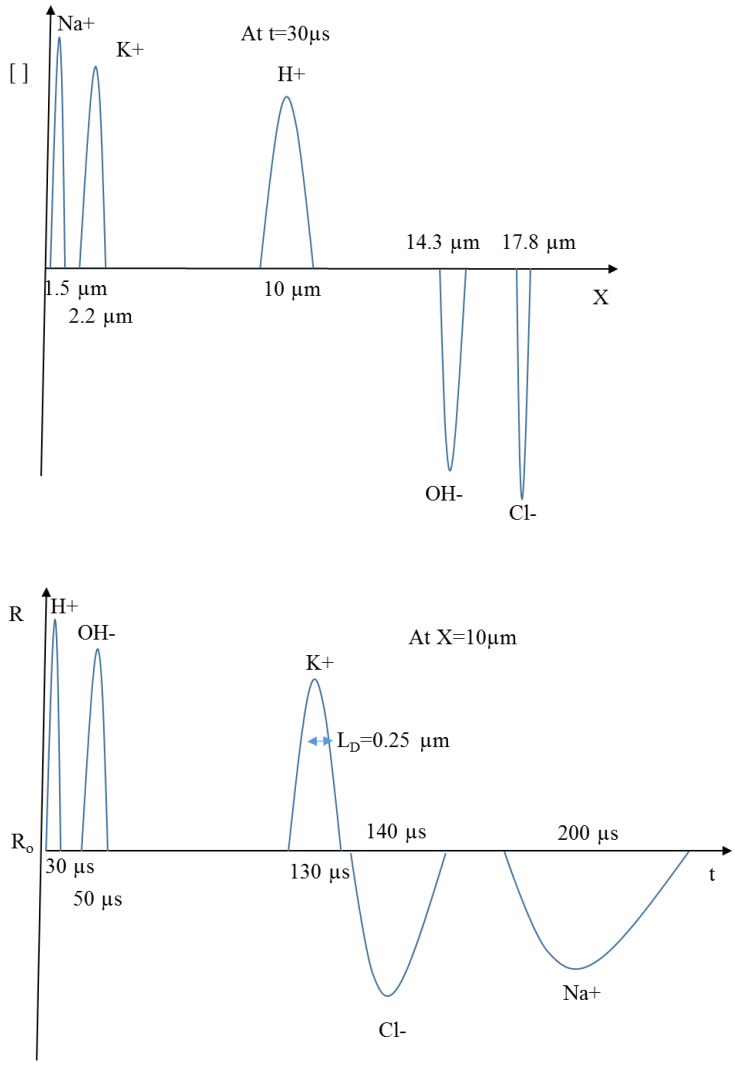

Figure 2.4 shows the spatial and temporal resolution of the species across the channel. The first graph shows the position of the species at time = 30 micro seconds. The second graph shows the temporal map at x = 10 microns. R_o is the quiescent resistance. The position of the nanowire is critical to be able to detect the species. Depending on the species of interest, a single nanowire or multiple nanowires can be designed to maximize ion separation, identification and measurement of concentration.

2.1.2.5 Advantages of the Dynamic Measurement System

The following discussion is not specific to the time-of-flight mode. Additional modes are introduced, as well as several features of this class of dynamic system which apply generally to the operation.

2.1.2.5.1 In Situ Cleaning of the Nanowire Sensor

One of the main challenges encountered in the glass electrode device is sensor drift over time. Park describes that the resistance versus time at a constant pH of 7 drifts about 10% over the course of 8 hours, figure [Park's graph]. This is a significant change in the response of the nanowire over time.

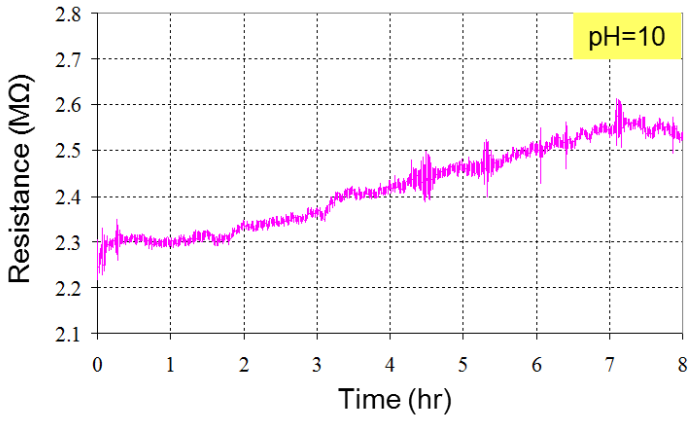

Figure 2.5 shows a graph of resistance versus time at a constant pH of 10. The graph shows sensor drift over time [Park]

The root cause of sensor drift is charged contaminants permanently adhering to the nanowire surface (not a part of the equilibrium reaction). To improve sensor drift over time, a special fluidic circuit could be designed to flush the nanowire sensor periodically but this will require a complicated fluidic arrangement. Other improvements are explored

in the present work and are detailed in chapter 4 using improved fabrication methods to minimize adhered charge. Another approach to periodic cleaning of the sensor is recognizing that the contamination of interest is necessarily charged in nature. An improved and simpler cleaning approach is to suspend measurement briefly and apply a periodic high external electric field perpendicular to the length of the nanowire sensor in order to electrostatically remove charge which are adhered to the nanowire. Then the electric field is turned off and the system is allowed to re-establish equilibrium before measurement resumes. This is a method for electrically cleaning the nanowire sensor in-situ without the need for complicated fluidic circuitry. This technique applies to the glass electrode system (with the addition of outer electrodes) as well as the dynamic system.

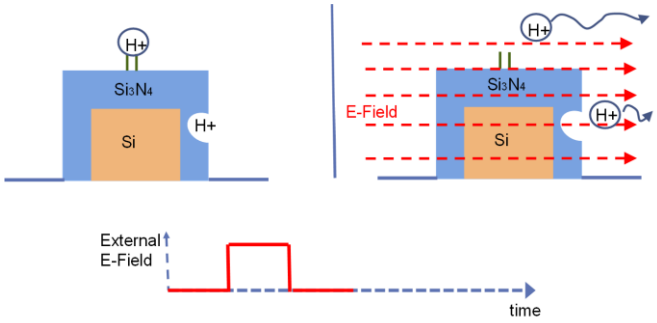

Figure 2.6 shows a cross sectional image of a nanowire sensor in a fluid. Ionic species present in the fluid, such as hydrogen ions, can get trapped or adhere at the surface of the nanowire as shown on the left, however, if an external electric field is momentarily turned on, these charges that are adhere at the surface can get be removed, improving the response of the nanowire and reducing sensor drift overtime.

2.1.2.5.2 Re-Zeroing the Nanowire Sensor

Another advantage of this dynamic system is a method to re-zero the sensor. After electrically cleaning the sensor as described above, some charges may continue to remain adhered at the surface. At this point, the fluid in the vicinity of the nanowire sensor is depleted of all mobile charge. The only charge that remains is stubbornly adhered parasitic charge. If an electrical reading of the nanowire is made immediately

after removing the cleaning electric field, but before equilibrium is re-established in the fluid and ions have sufficient time to diffuse back to the sensor, then this measurement is considered a new baseline reading for the sensor. Any permanently-adhered charges that remain at the surface of the nanowire sensor are effectively ignored, and fresh measurement of fluidic charge can be accomplished-- The contribution of any undesirable charge contamination is now subtracted from the resistance measurement using this method. This is also a major improvement in sensors of this type. This re-zeroing method is particularly important for the dynamic measurement, because in that sensor, there is, ideally, no adhered charge. In the case of the surface charge sensor (glass electrode), permanently adhered charge may serve to block potential binding sites, and therefore subtraction of the permanently bound charge may not completely eliminate the calibration error.

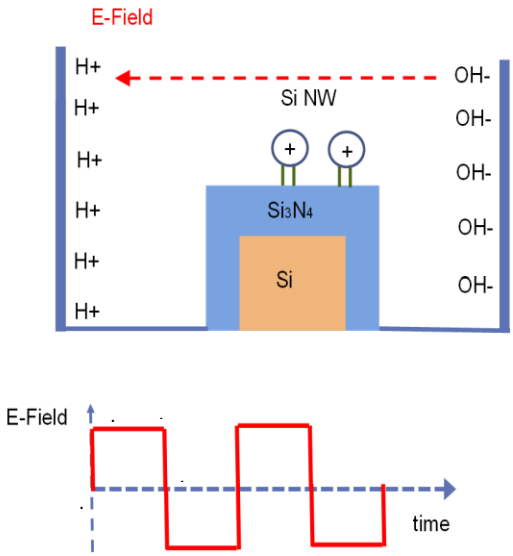

Figure 2.7 shows a cross-section of a nanowire sensor where ionic charges remain stuck at the surface after applying a high external electric field. A graph of the external electric field versus time is also shown. Notice that at t_0 the electric field is applied between the outer electrodes, at t_1 the positive ions in the fluid move to one side and the negative ions move toward the other side, collimating the ions and cleaning the sensor. at t_2 the electric field is reversed so ions from one side begin to migrate toward the opposite side in the channel and since the fluid is depleted of mobile ions, the sensor zero response

is established. At t3 the gaussian profile crosses the nanowire sensor and a dynamic measurement is performed.

2.1.2.5.3 Driving the Nanowire for Resistance Measurement

One of the challenges that are raised in this dynamic measurement system is the ability to maintain a uniform and constant external electric field to drive the ions via a drift mechanism across the channel. It is essential that this external electric field be uniform in order to maintain a constant drift velocity of each species, since $V=\mu E$. However, in order to sense a restistance change in the nanowire, the nanowire resistance must be probed by applying a potential difference along its length in the y direction and a current measured.

The application of a potential to the nanowire presents a problem when the nanowire is used in a dynamic system as described herein because the nanowire potential can disturb the uniform high external electric field and therefore disturb the species migration as they travel across the channel. The nanowire sensor effectively behaves as an additional electrode in the cell, thus perturbing the otherwise uniform potential created by the outer electrodes. To avoid such perturbations in the constant external electric field, several methods are presented in this work:

2.1.2.5.3.1 Pulsing the Nanowire Sensor

The first method consists of periodically measuring the species as they travel across the channel by momentarely pulsing the nanowire sensor. As a result, the potential between the outer electrodes is only perturbed breifly in time. This allows snapshots of the charge position discretized in time.

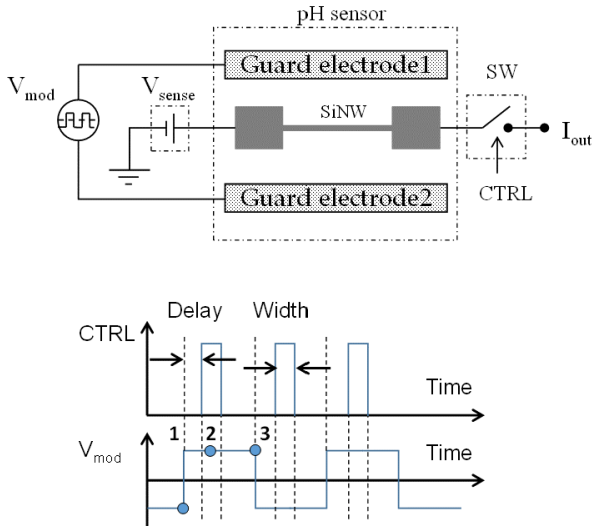

Figure 2.8 shows a schematic of a nanowire sensor in between two outer electrodes connected to a switch. When the switch is closed momentarily, the nanowire senses the species around it and allows the nanowire to make a measurement until the switch is open again.

2.1.2.5.3.2 Driving the Nanowire Sensor at the External Potential

A second method consists of carefully selecting the driving potential of the nanowire sensor, by matching the potential of the nanowire to the correct potential in the fluid as dictated by the outer electrodes. In other words, if the nanowire sensor is midway between the outer electrodes, then it should be driven at a potential that is an average of the two outer electrodes (between the channel) as shown in figure [2.2]. The method of driving the nanowire at a carefully selected potential can be combined with the method of pulsing the nanowire drive.

One problem that arises is that a perfect potential match between the nanowire and the fluid cannot be achieved because if the nanowire was driven at the same potential on both ends of its length then the nanowire will have zero potential difference across it, and the resistance measurement could not be done. The solution would be to drive the nanowire with a small change in voltage, that is, large enough that the nanowire senses the change in resistance but small enough to minimize the perturbation of the migration

of species across the channel. A solution to this challenge is shown on figure []. A series of resistors can be used around the nanowire to compensate for the potential drop, so that one end of the nanowire is at 5V for example and the other end is at 4.9 V.

A very small potential difference would lead to a very small sensed current, which would lead to more noise in the measurement.

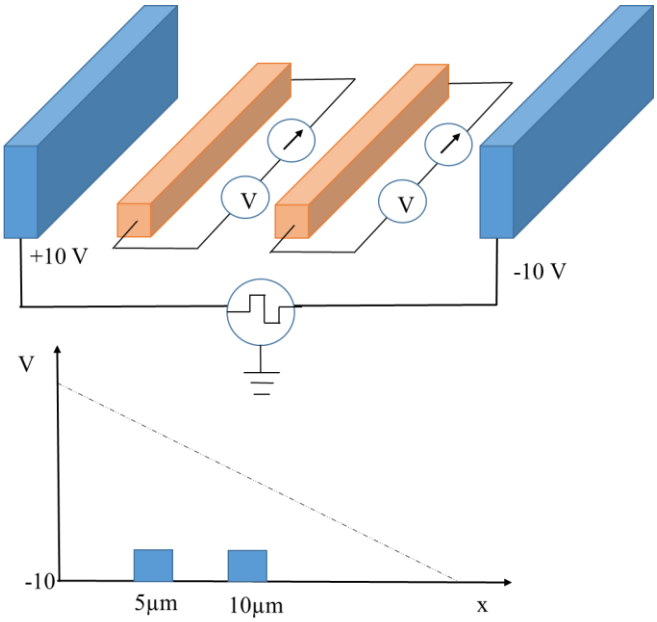

Figure 2.9 A system of nanowires sensors in between outer electrodes. The graph shows how the potential varies across the channel, so it is important to drive the nanowires at the correct potential in order to minimize the disturbance in migration of ions.

2.1.2.5.3.3 High Frequency AC Nanowire Drive

One of the problems with driving the potential difference along the length of the nanowire is that the nanowire causes a potential gradient of the high external electric field in the fluid along the y direction. This is a problem because the electric field gradient along the y direction of the nanowire will also cause a disturbance of the high external electric field in the same direction, therefore the species will not migrate evenly (at the same speed) along the y direction and may not approach the nanowire sensor at the same time, thus impeding the nanowire sensor from reading the true concentration of that particular species.

A third driving method for the nanowire is to use high frequency AC to probe the nanowire's resistance. The AC waveform is DC-offset to the correct potential, matching the predicted channel's potential at that point in space, but the potential varies rapidly around that DC-bias to determine the nanowire's resistance. The AC amplitude can be large, as long as the frequency is high enough that it does cause a net perturbation in the position of the ions.

2.1.2.5.3.4 Minimum Frequency AC

The minimum frequency required is a function of the ion mobility of the fastest ion, usually hydrogen. From Table 1.1, Hydrogen has a mobility of 360,000 um^2/Vs. If the AC frequency is 1MHz, a half-cycle of this waveform has a period of 1/2f = 0.5us. In that brief period, the migration of a hydrogen ion, assuming a constant perturbation to the constant electric field of 1V/um, would be $x=\mu*E*t = 0.18um$. This is a small motion of the hydrogen and would not perturb the reading.

2.2 Other Modes of Operation

In addition to the time of flight mode of operation described above, other novel modes of operation are also possible. The choice to employ different modes depends on the intended application, the species of interest, and interfering species that we wish to

measure or identify. Additionally, the measurement cycle time varies for different modes, and some modes are capable of a continuous measurement, and others must rely on cyclical processes. These modes of operation are intended to illustrate concepts. Detailed analysis of the time of flight mode is performed in Chapter 3.

2.2.1 Variable Frequency

For the purpose of description of this mode of operation, it is assumed that a test fluid contains four different species: sodium+, chlorine-, hydrogen+, and hydroxide- and the system has a p-type doped silicon nanowire.

Figure 2.10 shows a diagram of the response of the nanowire current versus frequency. Initially, shown in point 4, a signal on the outer electrodes is so in high frequency that none of the ions in the fluid can respond to it. The ions very slightly oscillate in place with total motion that is sub-micron. Thus, the ions are effectively evenly spread out in the channel and the nanowire response that is due to the charge of all the ions collectively, generally electrically balanced with equal concentrations of positive and negative charges. This response is effectively a zero reference corresponding to no depletion in the nanowire. At Point 3: the frequency of this signal is lowered and as a result the most mobile ions continue to oscillate in place, but higher mobility ions such as hydrogen are able to traverse the channel within the period of oscillation. This causes the nanowire resistance to momentarily decrease (current increases) during part of the period. The DC resistance component of the nanowire will have an increase in the resistance and the AC signal will emerge due to the periodic nature of the ions crossing it. Point 2: Suppose that the frequency is further lowered. This results in a negative ion such as Cl- now traversing the gap between the electrodes, as a result the magnitude of the AC signal will be increased but the DC current will decrease. This happens because the negative ion causes the resistance to momentarily decrease in the nanowire, unlike a positive ion which causes a momentary increase in resistance in the nanowire at a different point in the cycle. Point 1: If frequency is lowered even more then other ions that have lower mobility such as sodium for example will begin to travel in the channel and participate in the perturbation and the trend continues. Thus, this mode of operation shows how careful control of the frequency used in the operation of this dynamic device allows the ions of interest to respond in a way that the nanowire can measure their concentration.

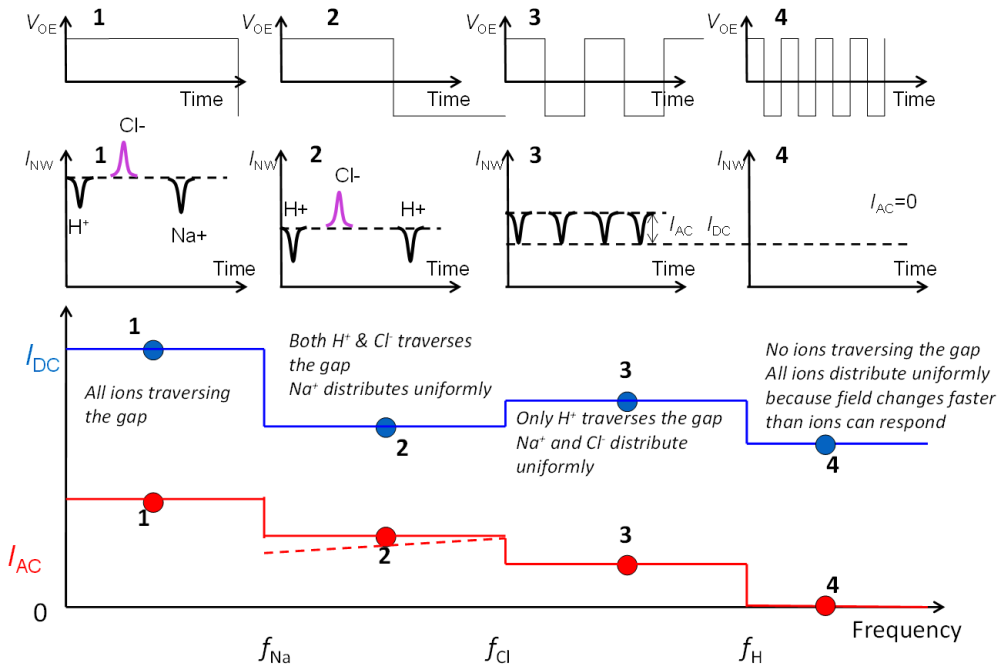

Figure 2.10 Response of the ions on the nanowire as the frequency is modulated

2.2.2 AC Modulation with DC Offset

The geometry of the system is similar to that for the variable frequency mode described above: a nanowire is placed in between two outer electrodes as shown in Figure 2.1.

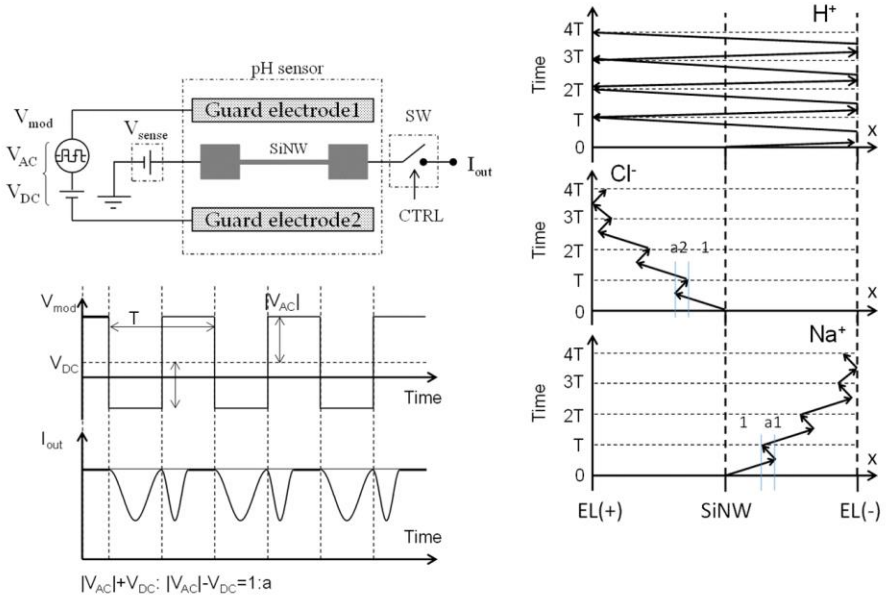

Figure 2.11 The large ion with less mobility displaces only a fraction of the electrode spacing and thus, migrates toward the opposite polarity electrode. The more mobile ion is able to transverse the gap from one electrode to the other in each cycle passing the nanowire sensor on each trip producing a momentary change in current in the p-type nanowire. The figure on the right shows a silicon nanowire (SiNW) in between two outer electrodes (EL), the Hydrogen ions transverse the channel on every cycle while the heavier ions migrate slowly toward the electrode.

Intially, if the outer electrodes are driven with a waveforms as shown in Figure 2.11, at a frequency of about 5 kilohertz with a DC offset, then the behaviour of a positive ion such as sodium will begin to drift toward one side and when the external electric field switches, the direction of the sodium ion will also begin to drift to the opposite direction. However, since the electric field is greater during one half of the cycle more than the other half, the net displacement of the sodium ion is toward the more negative electrode. Similarly, the behaviour of a negative ion such as chlorine will be similar to that of sodium except that the chlorine will have a net displacement toward the positive electrode. Over time, the positive ions in the fluid collimate against the negative electrode and negative ions collimate against the positive electrode. Once at the outer electrodes, the ions will “bounce” in and out of the walls in response to the dynamic external electric field. However, as the frequency is decreased (in this case, lower frequency allows more time for the ions to make it all the way across the channel)

hydrogen ions are able to migrate within one half cycle, to the nanowire and eventually across the entire channel. As a result, only hydrogen ions will cross the nanowire sensor. Therefore, a measurement of true concentration of hydrogen ions can be made while other ions remain isolated at, or near, the walls. If the frequency is lowered further, then other species begin to participate in the nanowire signal and the concentration of other species can also be made as they begin to cross the nanowire sensor. Thus, a method for measurement true pH and other species is shown with this mode of operation. Depending on the application, this mode of operation may be more advantageous to use. The amount of DC offset potential must be chosen large enough to retain the statistically fastest moving (diffusing) ions colimmated at the walls. Another variation on this mode Is to use, instead of a DC offset with ~50% duty cycle, a waveform that is equal in positive and negative potentials, but the duty cycle is asymmetric. (Figure showing asymmetric duty cycle). The operation is similar, but the modulation is performed with dissimilar positive/negative time in each cycle rather than variable positive/negative potential magnitues.

It is important to note that cell geometry is virtually unchanged in all of the modes described (time of flight, variable freq, DC offset/duty cycle), so all modes are possible with only a change in driving waveforms. Optimization of each design differs, but any mode can be employed once the cell is fabricated.

2.3 Summary of Chapter 2

In this chapter, a new class of pH sensor and ionic species discrimination system is intorduced. Nanowires are used as the charge sensor, however the system is not limited to this type of charge sensor. Various modes of operation and driving improvements are presented. In chapter 3, the preferred mode, the Time-of-Flight mode, is analyzed in greater detail.

CHAPTER 3. THEORY, MODELING AND SIMMULATION OF SPECIES DISCRIMINATION AND IDENTIFICATION

3.1 Analytical Models

The previous chapter illustrates how the operation of the dynamic ion sensor system is very dependent on the details of the dimensions and numerical constants. An important parameter to consider is diffusion of the ionic species in the fluid as they travel across the channel. Diffusion is difficult to suppress because diffusion is ever-present, seeking to spread the species concentration and making the species' measurement a true challenge. However, one advantage useful in this dynamic measurement system is that drift of the species is related to diffusion, therefore, the chosen value of the external electric field is critical because this value is directly proportional to drift velocity of the species. Another important value to consider is the distance between the outer electrodes and the nanowire sensor. This drift distance should be small enough so that drift velocity of the species dominates over diffusion but at the same time, this drift distance should be large enough to allow physical separation of the species that is to be measured. Therefore, it is critical to make a measurement fast enough to minimize diffusion. With this example in mind, numeric details of the system are calculated to find dimensions and operating conditions which allow a measurement to be made. It is clear that the cell must have microscale dimensions, necessitating nanoscale charge sensors, for mobilities of common ions in water solutions. As the following analysis proves, this system could not be duplicated on a macro-scale. This system is enabled by nanotechnology.

3.1.1 Ionic Concentrations and Initial Conditions

In a fluid sample in a cell volume, there exists a concentration of different ionic species. Seawater, for instance, contains roughly 28.0 g of (NaCl) per liter about 10g of Na and about 18g of Cl. This is equivalent to approximately 0.479 mols per liter [27]. At the same time the pH of water is near neutral, that is pH = 7 which, by definition, means that the H+ concentration is 10^{-pH}, that is, 10^{-7} mol/L. Given the dynamic system described in this work and upon application of the external electric field, the positive ions will migrate to one electrode and the negative ions toward the opposite electrode. For this analysis, it is assumed that initially the ions are essentially collimated against that

electrode (Perfect collimation is prevented by a double layer due to charge repulsion. An analysis of Debye length at the wall is discussed later).

3.1.1.1 Calculation of the Total Ionic Dose and Calculation of Areal Density Against the Electrode

In order to perform the analytical study, first, the total number of each species in the cell volume is calculated. By definition, pH is the negative logarithm base 10 of the hydrogen ion activity (H+) in solution which is shown in equation below

$$pH = -\log_{10}[H^+] \tag{4}$$

The units are in moles per liter [1]. This means that if the effective concentration of the species is known, then the pH can be calculated. For the analysis of the dynamic cell described in this work, using the physical dimensions of the cell (width, length and height), the volume is calculated, and converted to Liters. To calculate the total charge of hydrogen ions present in that cell, Equation (5) is used

$$Q(pH) = qN_A V_{volume} 10^3 10^{-pH} \tag{5}$$

Equation (5) is used because it describes the total number of charge as a function of pH where N_A is the Avogadros number in molecules per mole and q is the electron charge in Coulomb. Using the above Equation, the areal density or total density of hydrogen ions at the outer electrode can be calculated using Equation (6)

$$\rho_0(pH) = \frac{Q(pH)}{area * \varepsilon_r} \tag{6}$$

In this equation, ρ_0 is the delta function of the charge against the outer electrode in terms of the hydrogen ions per square meter (area) at the cell wall. It is the charge per unit area (areal charge density) corrected for the dielectric constant of water, and ε_r is the relative permittivity (dielectric constant) of water which is approximately equal to 80 at 20 C [28].

(The dielectric constant of water is very high because water molecules are highly polar with the hydrogen atoms positive and the oxygen negative. So water is good at shielding electric fields).

3.1.1.2 The Gaussian Profile

The total charge density can be calculated using two equations, one Equation is (6) and the other one is Equation (7)

$$\rho_{spatial}(x,t) = \frac{1}{a_H(t)\sqrt{2\pi}} e^{\frac{-(x-x_0(t))^2}{2a_H(t)^2}} \quad (7)$$

Where $\rho_{spatial}$ is the Gaussian (normal) distribution, x_o is the mean and a is the standard deviation [29] which in this case a is described in Equation (8)

$$a_H(t) := \sqrt{D \cdot t} \quad (8)$$

Where D is the diffusion coefficient and t is time.

Equation (7) is normalized and depends on x and t, thus it provides spatial and temporal distributions but not pH or charge. Equation (6) depends on pH and doesn't provide with any spatial nor temporal distribution of ions. Thus, to calculate the total charge density as a function of x, t, and pH both equations (6) and (7) are combined

$$\rho(x,t,pH) = \rho_0(pH)\rho_{spatial}(x,t) \quad (9)$$

Thus, looking at a cross section of the channel, the total number of hydrogen ions can be calculated as shown in the graph below. This will be the same for z and y values.

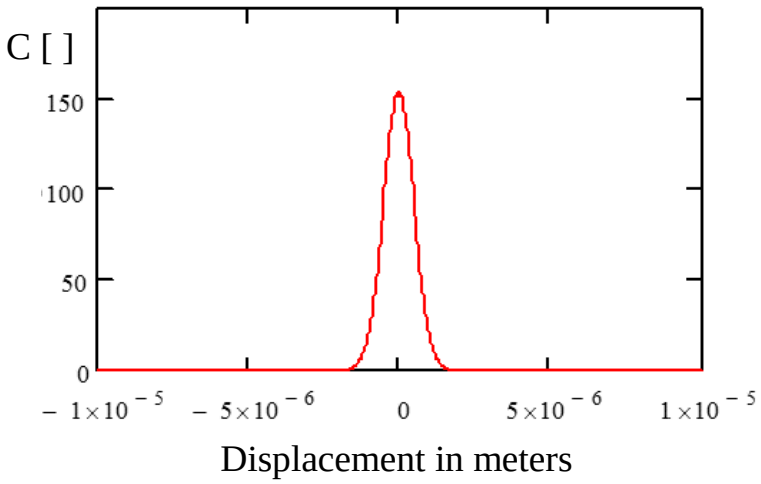

Figure 3.1 showing the Gaussian profile formed after calculating the total number of hydrogen ions in moles per cubic meter with pH = 7

Given this charge concentration, the electric field can be calculated at the surface of the nanowire sensor. More details are described in section 3.1.3

3.1.2 Drift-Diffusion

As discussed earlier, one of the main challenges in this type of sensors is diffusion because it spreads the species in space and can disturb the measurement, however, the advantage is that diffusion is dependent on drift, and as seen in Equation (1), drift is proportional to the external electric field which can be easily controlled. Therefore, the species travelled by a controlled velocity. The drift-diffusion analysis in this work assumes that the species travel at a terminal velocity proportional to the external electric field. However, the species initially collimated at the outer electrode, begin drifting from rest, therefore, there is some acceleration period before they reach constant velocity. Thus, is constant velocity a reasonable assumption?

The answer to this question both fluids and terminal velocity analysis in the fluid is discussed.

It is important to discuss why terminal velocity can be assumed for this analysis. To recall the reader, the ions are initially collimated against the outer electrode. Naturally, this forms a Debye layer at the outer electrode, therefore, let's first analyze the Debye length [30].

Assuming a neutral solution with pH = 7 and using Equation ()

The Debye length is calculated showing a kappa in the nanometer regime [31]. Therefore, the Debye length is significantly less than the diffusion length calculated for the Gaussian profile which is about half a micron for hydrogen after traveling for 30 microseconds. It is interesting to note that as the pH increases, the Debye length gets thicker. This is not desirable because the ions are no longer collimated against the wall, but instead the ions begin to move with an already spread profile as if they are already initially diffused. The key is to reduce the effect of diffusion to obtain a profile of the species around the nanowire that has a sharp peak to make an accurate measurement. Nevertheless, as the pH increases and the Debye length thickens at the wall, the concentration of OH can be measured instead providing accurate pH measurement results.

Next, to calculate the time it takes an ion to achieve terminal velocity, creeping flow is assumed, that is, the inertia forces of the fluid can be neglected and the Reynolds number (the ratio of inertial to viscous forces) is much less than one (no turbulence) [32]. Using Stokes' law, the sum of the forces becomes Equation (10)

$$F = ma + qE + 3\pi\mu dV \tag{10}$$

Where μ is the mobility of the ion, d is the diameter of the ion and V is the velocity.

$$V_f = V_i + at \tag{11}$$

And Equation (11) is used where the initial velocity is assumed zero (the ion starts moving from rest).

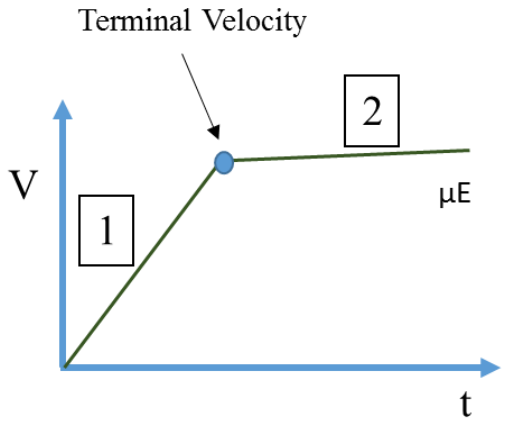

Figure 3.2 Velocity versus time. The graph shows two regions. Region 1, where the ion accelerates and region 2 where the velocity of the ion has plateau. The point where Region 1 and Region 2 meet is the terminal velocity, the parameter of interest in this section.

Two regions can be considered as in Figure 3.2 above: region 1 describes the acceleration of the ions, that is, as soon as the voltage at the outer electrode is reversed, the ion begins to accelerate, so friction is neglected. Using the two equations above and simplifying, Equation (12) is shown

$$V(t) = \frac{qE}{m}t \qquad (12)$$

In region 2, the velocity of the ion plateaus (so acceleration in Equation (10) is neglected and friction becomes important),

$$qE = 3\pi\mu dV \qquad (13)$$

$$V = \mu E \qquad (14)$$

$$t = \frac{V}{a} \qquad (15)$$

In addition, velocity equals the mobility of the ion times the electric field [33].
To find terminal velocity, region 1 is equated to region 2. Solving for time, hydrogen ions achieve terminal velocity in approximately 3.7 femtoseconds and sodium ions in approximately 12 femtoseconds. Therefore, terminal velocity can be assumed when performing the following analysis below.

3.1.3 Electric Field Calculation due to the Centered Ionic Charge Concentration in the Fluid

This analysis of the electric field is for a Gaussian distribution of Hydrogen ions (one species) centered around the nanowire along the x axis. The centered Gaussian is the condition of most interest because that is where the signal is maximum. First, the electric field is calculated due to a centered Gaussian profile using Coulombs law. Coulombs law states that "The magnitude of the electrostatic force of interaction between two point charges is directly proportional to the scalar multiplication of the magnitudes of charges and inversely proportional to the square of the distance between them" [34]. If the two charges have the same sign, then they repel each other and if the charges have opposite signs then they attract each other. Coulomb's law can also be described mathematically using the vector Equation (16)

$$F = k\frac{q_1 q_2}{r^2} \tag{16}$$

Where k is the Coulomb's constant, q_1 and q_2 are the magnitudes of the charges and r is the distance between the charges. The electric field is the Coulombic force experienced by a charge. This force on a charge depends on the strength and direction of the electric field as shown in Equation (17)

$$F = qE \tag{17}$$

Since the electric field is a vector, then the calculation must integrate over the entire volume of the cell, in x, y and z; however, since the ionic charge Gaussian profile is

centered around the nanowire sensor, there is both y and x symmetry at this point, thus, the resultant field will only have a z component, so the calculation can be simplified from a vector integral to a simple scalar integral for this case. Later on, section 3.2.7 shows the analysis of an arbitrary Gaussian profile off-centered with respect to the nanowire. The analysis in that case is more complex since both the x and z components of the electric field have to be taken into consideration. However, for now, symmetry allows the calculation to be simplified using the z component of the electric field only.

Given the charge distribution shown in previous section, the z component of the electric field at the surface of the nanowire sensor is given by the triple integral as follows:

$$E_z(pH) = \int_{\frac{-w}{2}}^{\frac{w}{2}} \int_{h_0}^{h} \int_{y_1}^{y_2} \frac{k\rho(x, y, z, pH)}{x^2 + y^2 + z^2} \frac{z}{\sqrt{x^2 + y^2 + z^2}} dydzdx \qquad (18)$$

Where the limits of integration in x assume the nanowire sensor to be in the middle of the channel (at 10 microns)

The solution for this triple integral can be done analytically for two of the dimensions but the Gaussian integral has to be performed numerically. The magnitude of this electric field is the quantity that yields the individual species concentration in the test fluid.

There is a thin dielectric (nitride) surrounding the nanowire to prevent charge transfer (electrochemical reactions) between the fluid and the semiconductor [25]. Mathematically, this is accounted by two ways: one way is by the limits of integration in the fluid (h_0 is the height of the nanowire). Once the integral is solved, the electric field in the surface of the nanowire is calculated. This electric field result at the surface of the nanowire is translated through the insulator in the semiconductor. Gauss law must be used to translate because what is constant in the insulator and through the semiconductor

is the electric field displacement. There are no charges present in the insulator. Thus, the electric field at the surface of the semiconductor can be calculated [35].

Since the electric field is constant inside the insulator material, the electric field displacement relation can be used as shown in Equation (19) in a region absent of charge and calculate the depletion region.

$$D = \varepsilon E = \text{constant} \qquad (19)$$

3.1.4 Resistance Depletion Analysis

Given the electric field calculation shown in previous section, the depletion region can now be calculated using Gauss law [36].

$$x_{dep}(pH, N_a) = \frac{\varepsilon_{si}\varepsilon_0 E_x(pH)}{N_a 100^3 q} \qquad (20)$$

Where ε_{si} is the dielectric constant of silicon and ε_0 is the permittivity of free space. N_a is the doping concentration.

Since the depletion region has been calculated above, the resistance in the nanowire can be calculated [37] from Equation (14)

$$R = \frac{\rho L}{A} \qquad (21)$$

Where R is the resistance in the nanowire, ρ is the resistivity of the material (Silicon), L is the length of the nanowire in the y direction and A is the cross-sectional area of the nanowire sensor. ρ and L are constant but what is changing is the cross-sectional area. The reason why the area changes is due to the formation of the depletion region. When the holes in the semiconductor move away from the periphery of the semiconductor (in the presence of positive ionic species such as Hydrogen) they leave behind negatively charged electrons, then due to Shockley Read Hall (SRH) recombination, the holes in the semiconductor recombine with electrons to restore equilibrium, that is $np=n_i^2$ must be true [38]. When the cross sectional area decreases, the resistance increases and this resistance corresponds to a particular pH [25]. ,

The pH scale is generally referred to being measured from 1 to 14 which is 14 orders of magnitude!! Since pH is represented on a log scale then 1 to14 represents 10^{-1} to 10^{-14} which is 14 orders of magnitude. This represents a huge dynamic range problem. (Analogous to the distance from earth to the sun measured in millimeters)
However, one advantage of working with semiconductors is that doping can easily be changed; in fact, doping can easily be varied by 7 orders of magnitude. By changing this doping the dynamic range can be increased allowing a wider measurement of pH range.

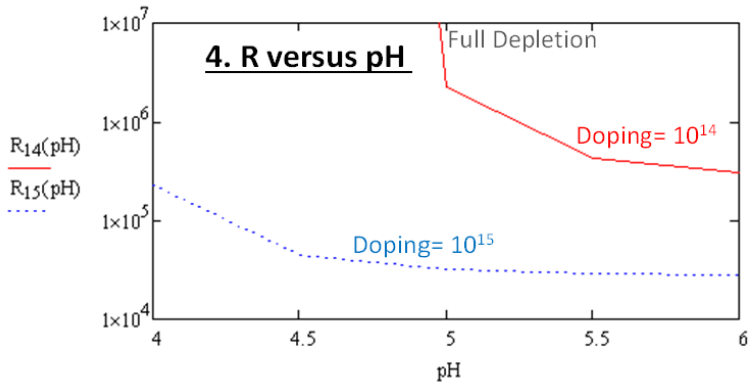

Figure 3.3 Each curve shows three regions. The solid curve show how the resistance goes to infinity indicating that the nanowire has reached full depletion, on the right side of the curve where is flat, around pH 6, the curve is asymptotic (it planes out indicating poor sensitivity) so the region of interest is the middle region between these two extremes.

3.1.5 Sensitivity Analysis

Sensors are giving out an electrical response due to a change in a physical quantity. One important aspect of sensors is their ability to sense the quantity that they are designed for. Sensitivity is usually defined as the output to input ratio. In this work, sensitivity is defined as Equation (22)

$$\frac{\frac{\Delta R}{R}}{\frac{\Delta pH}{pH}} \qquad (22)$$

Another important parameter in sensors is the range at which the sensor operates. Every sensor is designed to work over a certain range. However, as shown in graph (below), changing the doping in the semiconductor extends the dynamic range and allows the dynamic system to sense pH over a wide range.

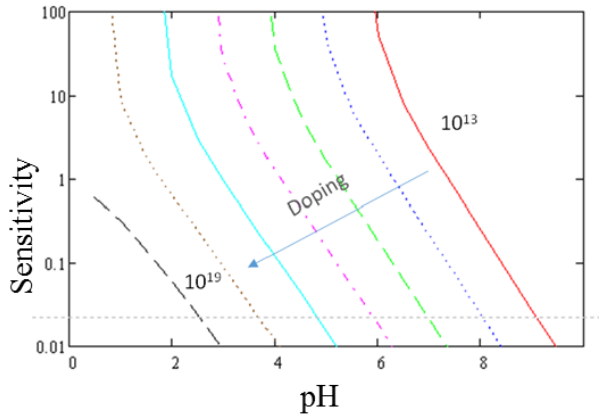

Figure 3.4 Sensitivity versus pH. Changing the doping in the semiconductor allows the sensor to measure over a wide range of pH, so depending on the application, the semiconductor can be doped accordingly to sense the desired pH.

3.1.6 Off-Centered Concentration Profile Analysis

3.1.6.1 Off-Centered E-field Analysis

In this section, the response of the nanowire is calculated for a Gaussian charge profile which is not centered over the nanowire. The analysis provides the off-peak response, but more importantly, the electric field affecting the nanowire is now a vector not purely in the z-direction. This analysis is important for calculating the interference of other ions. For example, when true pH is sought in a salt water solution, how much influence does the off-center sodium have on the centered hydrogen peak response?

This analysis assumes that a channel size is 20 microns and the nanowire sensor is at the center of the fluidic channel. First, an analysis is done of a single species (H+) travelling in time along the channel. When the ions drift toward the opposite electrode

in response to the change in potential of the outer electrodes, hydrogen ions begin to drift and diffuse as they propagate across the channel.

To calculate the electric field, the same Gaussian pre-factor is used as in Equation (6). The term $x_0(t)$ is given by Equation (23)

$$x_0(t) = \mu_H E t \qquad (23)$$

Where μ_H is the mobility of hydrogen ions. Next, the electric field calculation precedes as before although the symmetry is now not present in the x-direction. There is still symmetry in the y-direction, and a triple integral must still be performed, but the integral is now a vector integral because the resultant field will now have both x and z components. The z component and the x component of the electric field must be considered in the off center analysis. The y component of the electric field is zero both in time and space due to symmetry. A triple integral is solved for the z component of the electric field and a triple integral is also solved for the x component of the electric field separately.

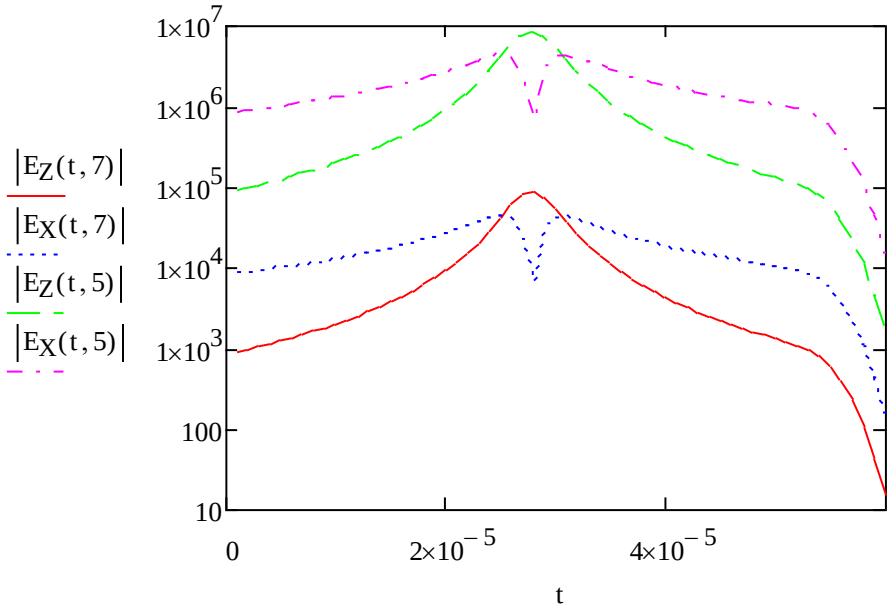

Figure 3.5 shows the z and x components of the electric field as a function of time for hydrogen ions travelling across the channel for two different pH.
Notice that the x component of the electric field drops at the center of the nanowire sensor. This shows that when the hydrogen ions are centered around the nanowire, the x component of the electric field cancels due to symmetry and only the z component affects the nanowire sensor. This result is consistent with the previous analysis.

3.1.6.2 Calculation of the Sensor Response with Vector Fields (off-center analysis)

The depletion region in the nanowire is calculated just like in previous section but for both x and z regions. Therefore in this case, there is a depletion region due to the x component of the electric field and a depletion region due to the z component of the electric field as in Figure 3.6

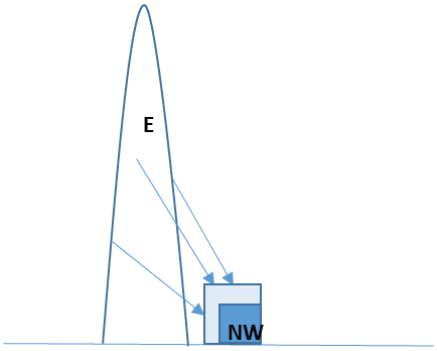

Figure 3.6 shows an off-centered Gaussian profile of ionic species which causes a depletion region on the nanowire both on top and on the side

From the depletion region, the total change in resistance due to both x and z components is calculated using a z component equation similar to Equation (20).

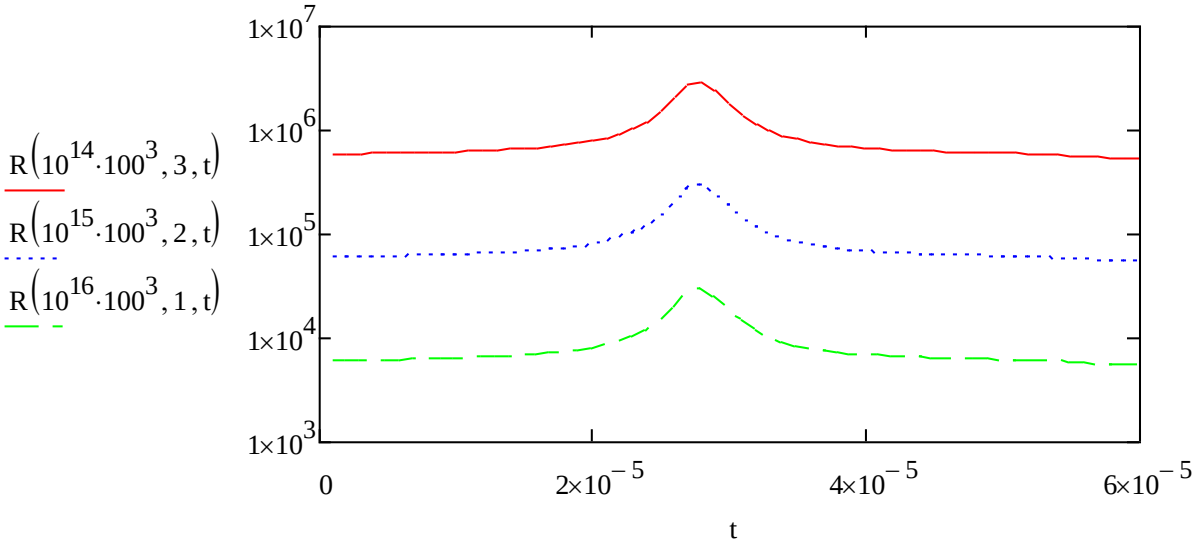

Figure 3.7 The response of the nanowire versus time at various doping concentrations

A comparison between the resistance due to the z component only and the total resistance (including z and x components) is also analyze as shown in Figure 3.7. An interesting point here is that when the nanowire is wider, it depletes more on the sides, therefore,

making the nanowire sensor more sensitive

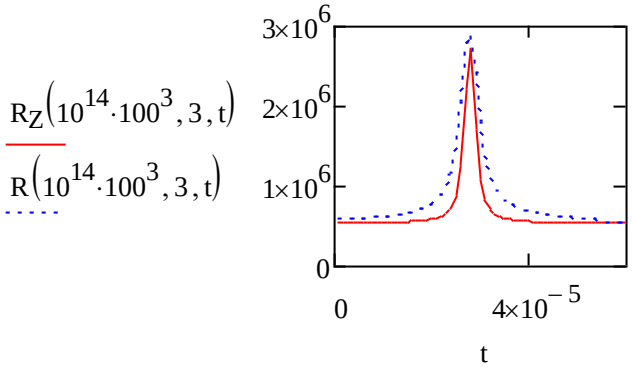

Figure 3.8 shows the difference between a nanowire where the x component of the electric field has been blocked shown with a solid line and where the x component of the electric field has not been blocked shown with dash lines. The difference is more significant as the width is made smaller because width controls the sensitivity to the x component of the electric field and height controls the sensitivity to the z component.

A more interesting analysis is the off centered analysis when two species are present. Let's assume that in addition of hydrogen ions, another positive ion such as sodium is present in the fluid and let's assume that the cell is the same as described above. The following analysis describes this situation.

The calculation of the electric field follows the same guidelines as in previous section including this time the z and x components for the off centered analysis. The electric field due to these two components versus time for sodium ions in pH 5 fluid is shown in Figure 3.9

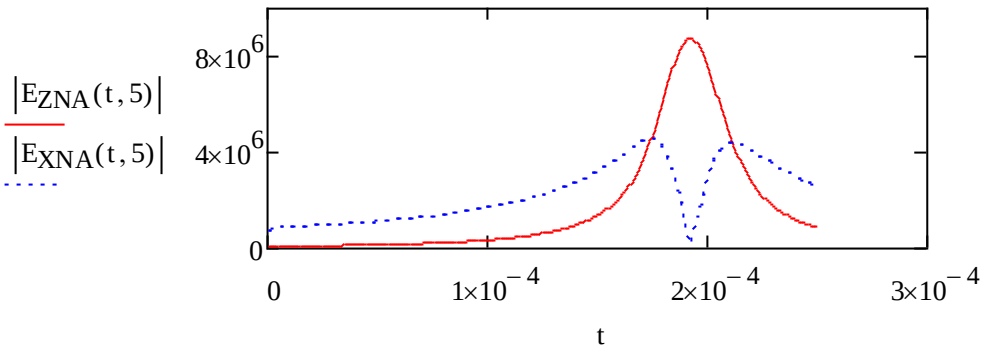

Figure 3.9 Electric field versus time of sodium ions in a fluid with pH 5. It is shown that the x component of the electric field drops as it approaches the center of the nanowire sensor.

Then the total electric field due to both species is calculated and shown on Graph ()

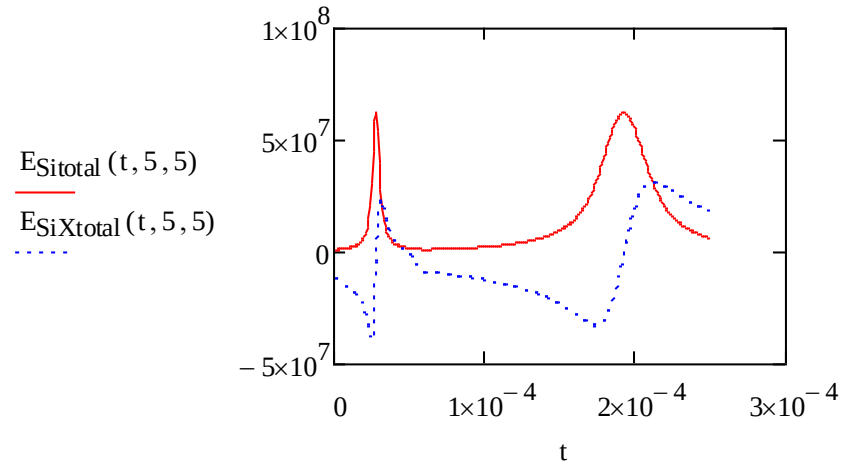

Figure 3.10 describes the comparison between the total electric field due to both species and the electric field due to the x component of the two species only

From the electric field, the depletion region and the total resistance on the nanowire sensor can be calculated as shown before.

Figure 3.11 shows the depletion region in the nanowire due to both species present. As a result of the sodium concentration present in the vicinity of the nanowire, a depletion region due to the sodium is observed on the nanowire, leading to ion interference.

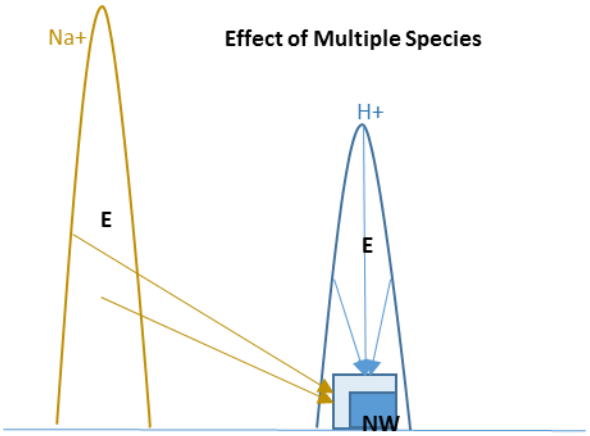

Figure 3.11 describes the depletion region on the silicon nanowire sensor from two different species. The hydrogen ions deplete the nanowire in the z direction (from the top) and the sodium ions deplete the nanowire from the side (in the x-direction). This has an effect on the resistance change in the nanowire, thus, shielding the nanowire sensor from the x-direction provides a more accurate measurement.

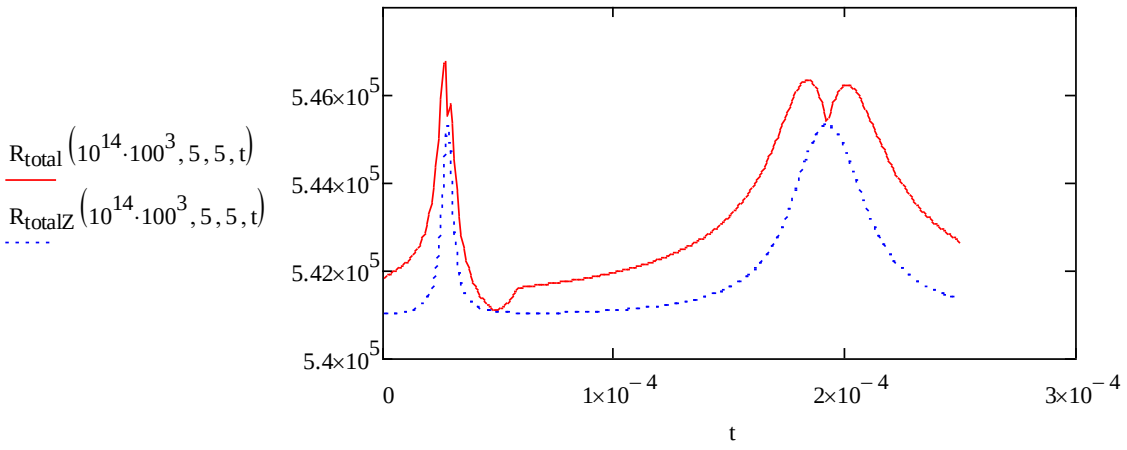

Figure 3.12 shows the comparison between the total resistance due to x and z components and the resistance due to the z component only versus time.

When the x and z components are both present the profile becomes more smeared.

An interesting aspect from this analysis is that the sodium will clearly have an effect on the hydrogen response of the nanowire. When the hydrogen ions are centered around the nanowire and the signal is maximum, the nanowire will also see the sodium due to a depletion region caused from the x component of the electric field from the sodium ions. Therefore the total resistance change in the nanowire will be due to both species leading to an erroneous measurement of true pH. An improvement to minimize the effect of other species interfering the nanowire reading is to block the x component of the electric field. By blocking the x component of the electric field, the nanowire is shielded from the sides and only the z component of the electric field causes a depletion region from the top of the nanowire. This is an important contribution because it helps to measure the true concentration of pH and also it helps with ion interference.

3.1.7 Dynamic Range

When designing a sensor, dynamic range is important because it determines in what conditions the device can operate and for what applications it can be used. Dynamic range determines the smallest and largest values of a changeable quantity. Earlier, it was described that pH is normally considered between 1 and 14 which is 14 orders of magnitude. This presents a true dynamic range challenge. However, in addition to doping the nanowire sensor as mentioned in the previous section, other alternatives can be considered and can be applied to increase the dynamic range of this dynamic sensor. These ideas are proposed and described below

3.1.7.1 Retrograde Doping Profile

In the case where only a single nanowire sensor is desired as opposed to using an array of multiple nanowire sensors along the channel, a retrograde doping profile nanowire sensor can be useful to increase the dynamic range. Using multiple ion implantations and a diffusion process, the nanowire can achieve a retrograde doping profile as shown in Figure 3.13. The advantage is that heavy doping around the periphery of the nanowire sensor is useful to sense higher pH. As the nanowire depletes, then

lighter doping at the core (or vice versa) can be used to sense lower pH.

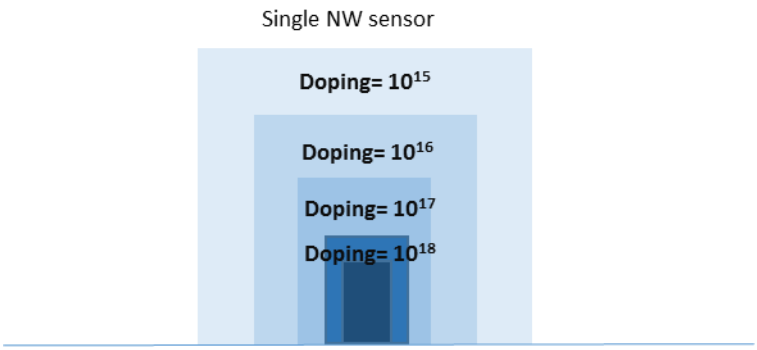

Figure 3.13 shows a silicon nanowire with a retrograde doping profile. This allows a dynamic range advantage.

3.1.7.2 Scaling of the Nanowire Size

In previous section, it is shown that the nanowires deplete from both the sides and the top. The range on the nanowire is limited by the amount of depletion. Therefore, if the nanowire is fully depleted then there is no more range and the nanowire cannot measure beyond that point. Another parameter that can be used to increase this limitation is the width of the nanowire sensor. Equation (14) shows how the change in resistance of the nanowire is inversely proportional to the cross sectional area. As the height and width change, the resistance changes. When the width goes to zero, the cross-sectional area goes to zero and the change in resistance goes to infinity. Sensitivity on the other hand is given by Equation (), so as the resistance becomes larger, then sensitivity also increases. Therefore a narrow nanowire will be very sensitive but it will be fully depleted very quickly. If the nanowire is made wider by increasing the width, then the range will increase but the sensitivity will go down. A wider nanowire is also useful when choosing a retrograde doping profile nanowire as described above.

3.1.7.3 Complementary Nanowire with Opposing Doping Profiles

One advantage to increase dynamic range is the fabrication of nanowires with opposing doping profiles. The nanowires studied in this work are all p-type. However,

nanowires with n-type doping can also be fabricated and studied along with the p-type nanowires. Instead of having a depletion region in the presence of a positive ion, the n-type nanowires will be in accumulation leading to a change in resistance as well. This can be advantageous when measuring certain pH ranges.

3.2 Modeling and Finite Difference Analysis of Silicon Nanowire Sensors for Ionic Species Identification

This dynamic system of silicon nanowires for ion identification can be modeled by a finite-difference method using drift-diffusion partial differential equations. This allows to study the behavior of the ions as they migrate from one outer electrode to the other in the presence of an electric field. Assuming a fluid that contains hydrogen ions, the partial differential equation is given by Equation (24):

$$\frac{dC}{dt} = D\frac{d^2C}{dx^2} - V\frac{dC}{dx} \tag{24}$$

Where C is the concentration of the species in the fluid, D is the diffusion coefficient and V is the drift velocity (or velocity of the fluid).

Using the finite difference approximation, the values for Δ x and Δ t are set as follows:

$$\Delta x = x_i - x_{i-1} \tag{25}$$

$$\Delta t = t_j - t_{j-1} \tag{26}$$

This method is fully implicit in order to guarantee stability
It is assumed that

$$\frac{D}{\Delta x} > \frac{V}{2} \tag{27}$$

This allows the function to converge, and another assumption is V>0

$$C(x_i, t_j) = C_{i,j} \tag{28}$$

Where i=1..M and j=1..N and M and N are the number of steps.
Using difference quotients, the partial differential Equation (24) becomes

$$\frac{C_{i,j+1} - C_{i,j}}{\Delta t} = D\frac{C_{i+1,j+1} - 2C_{i,j+1} + C_{i-1,j+1}}{(\Delta x)^2} - V\frac{C_{i+1,j+1} - C_{i-1,j+1}}{2\Delta x} \tag{29}$$

Rearranging the equation above, the following tridiagonal system of linear equations are obtained:

$$(\frac{-D}{\Delta x} + \frac{V}{2})C_{i+1,j+1} + (\frac{\Delta x}{\Delta t} + 2\frac{D}{\Delta x})C_{i,j+1} + (\frac{-D}{\Delta x} - \frac{V}{2})C_{i-1,j+1} = \frac{\Delta x}{\Delta t}C_{i,j} \tag{30}$$

In addition, let

$$a_E = \frac{D}{\Delta x} - \frac{V}{2} \tag{31}$$

$$a_W = \frac{D}{\Delta x} + \frac{V}{2} \tag{32}$$

$$a_{p0} = \frac{\Delta x}{\Delta t} \tag{33}$$

$$a_p = a_{p0} + a_E + a_W$$

Then the linear equation becomes:

$$-a_E C_{i+1,j+1} + a_p C_{i,j+1} - a_W C_{i-1,j+1} = a_{p0} C_{i,j} \tag{34}$$

The linear equations are solved by using a Thomas algorithm to obtain an approximate solution to the drift-diffusion partial differential equation [39].

The result is the concentration as a function of displacement (x) and time (t), that is, it shows how the concentration across the cell, from x=0 to x=L, changes with time due to the drift and diffusion of the ions as they travel across the channel in the presence of an electric field.

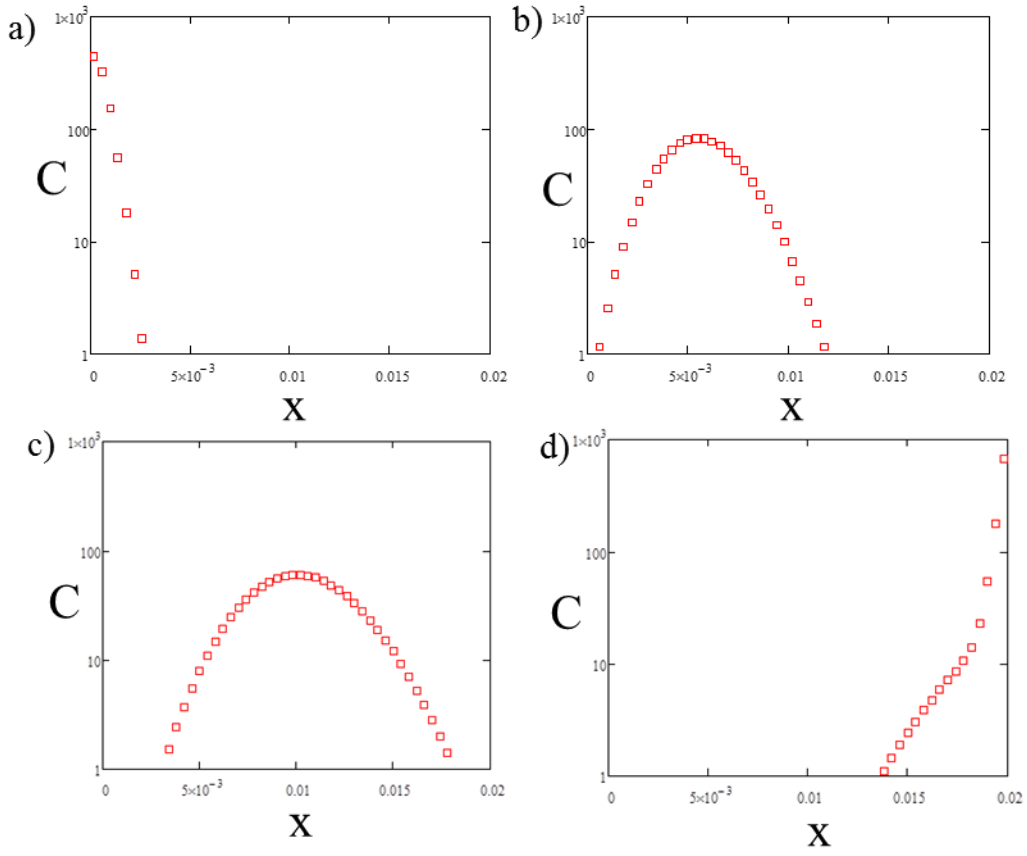

Figure 3.14 shows four different graphs of the hydrogen ion concentration moving across the fluidic channel as a function of time and space. The channel is 20 microns long and the nanowire sensor is assumed to be in the middle of the channel. Graph a) shows the concentration of hydrogen ions at time 5Δt, just after the ions leave the outer electrode. Initially, the ions are collimated against the outer electrode eliminating the effect of diffusion. This allows a sharper peak when the ions arrive at the

nanowire sensor. Graph b) on the top right shows the concentration of hydrogen ions at time 90Δt. Graph c) shows the concentration of hydrogen ions at time 165Δt. Notice that as the ions drift, they also diffuse. This is represented by the Gaussian profile. Graph d) on the bottom right shows how the ions collimate as they approach the outer electrode.

The results from this modeling work are consistent with the analysis done by analytical methods shown earlier in this chapter. In addition, the values of the diffusion length or amount of spread of the Gaussian shown in this modeling are also consistent with those shown using analytical methods. See table below for more details (Let t = 30 microseconds).

Parameter	Modeling	Analytical
Location of H+ in channel	11.2 microns	10.8 microns
DiffusionCoefficient $L = \sqrt{Dt}$	0.55 microns	0.53 microns

Table 3.1 shows a comparison in results between the modeling and theoretical analysis. The results are consistent.

CHAPTER 4. FABRICATION OF SILICON NANOWIRES FOR IONIC SPECIES DISCRIMINATION AND IDENTIFICATION

The analysis in the previous chapter indicates that species separation and identification works best when the dimensions of the nanowires are small. Indeed, diffusion would convolute any separate measurement of many common ionic species if drift distances were larger than perhaps a few hundred microns. Researchers in previous work have used nanowires for sensing mainly due to advantages in sensitivity because of a large surface-to-volume ratio [18]. In this work, nanowires are used not only because of this sensitivity but also because of the small size is able to resolve the spatial location of charge in a cell having dimensions on the micron scale. The small cell is required in order to minimize diffusion in the fluid and also to have a low Reynolds number to avoid turbulence in the fluid. This work uses a top down process with a SOI silicon wafer. The process is subtractive and the nanowires are formed in the SOI device layer. This method was chosen as the most robust method for deterministic placement of the nanowires, extremely smooth sidewalls and repeatability which are difficult in the bottom up processes. However, as bottom-up processes are improved and made more repeatable, these higher-performance structures can easily be integrated into the sensor system presented herein. Top down fabrication is merely chosen as more practical for demonstration of the overall system and concepts at this time.

In this chapter, the state of the art nanowire fabrication process is improved. First, some causes of major known issues are identified and improved. Then an integrated nanowire process is presented. Finally, a complete dynamic cell with nanowire sensors is presented as a two-wafer, bonded process.

4.1 Challenges in Existing State of the Art Processes

After forming the nanowire sensor, a dielectric film is deposited around the nanowire in order to encapsulate the sensor to electrically isolate the nanowire from the surrounding fluid. This prevents charge recombination at the wire-solution interface. This dielectric is necessarily very thin (a few nanometers) so that the electric field penetrates from the solution into the nanowire causing charge carrier depletion in the semiconductor, but it needs to be thick enough to prevent charge transfer (by tunneling or leakage) between the semiconductor and the fluid.

If this film is not perfectly conformal or has varying thickness over the nanowire sensor, then it can lead to an erroneous measurement. In the case where the film doesn't completely isolate the nanowire (a pinhole), charge is able to transfer between the fluid and the semiconductor, and the nanowire behaves as an electro-chemical cell. In the case where the film only partially covers the nanowire (poor conformality), quantum mechanical tunneling of charge carriers through the thinner dielectric would also cause electrical leakage. Pinholes can also lead to an ion or charge being trapped or immobilized within or on the surface of the dielectric, therefore causing the sensor response to drift over time as the charge is erroneously trapped and released. Neither case is ideal [40, 41].

The root cause of pinholes in the state of the art fabrication process is the Plasma Enhanced Chemical Vapor Deposition (PECVD) process used for depositing the dielectric film surrounding the nanowire [25, 26]. PECVD is deposited at a lower temperature (~350 C), compared to low pressure chemical vapor deposition (LPCVD), which is performed at higher temperature (~800 C) [42]. The reason that PECVD was used by Park instead of the higher temperature process is because of the chromium used in the prior hardmask step. Any residual chromium remaining would be diffused into the silicon (and the process equipment, eventually contaminating subsequent wafers processed therein). Chromium is known as a deep-level electronic trap in the silicon bandgap, causing junction leakage and electron-hole pair recombination. Any processing steps following the chromium deposition are kept to low temperature for this reason.

PECVD provides good adhesion and uniformity and most importantly for that

process, low deposition temperature (~ 350 C) compared to other chemical vapor depositions (CVD) methods. PECVD allows a large choice of materials to be deposited such as silicon nitride and silicon oxide. However, PECVD generally produces a films with higher pin hole density when compared to other higher temperature deposition methods such as low pressure chemical vapor deposition (LPCVD) [42]. Therefore, a process that can withstand higher temperatures is highly desirable. This can be accomplished by either eliminating the use of chromium, or rearranging the chromium step to occur later in the process. The redesigned, integrated process shown later in this chapter removes the chromium hardmask entirely from the process.

4.1.1 Line Edge Roughness

An ideal nanowire has smooth, straight walls. When line edge roughness (LER) is present, the nanowire looks like the one shown in Figure 4.1 and Figure 4.2. Line edge roughness is not ideal because the cross sectional area of the nanowire along its length varies, therefore the resistance is not uniform along the length of the nanowire sensor. Even worse, as the semiconductor nanowire is depleted of charge around the periphery, the change in resistance (or, stated another way, the area not depleted) varies much more along the length when the LER is large. This presents a problem because now the nanowire behaves like distributed series resistors each having different values depending on their cross-sectional area. The regions having smaller cross-sectional areas will have a larger change in resistance given the same surface charge compared to the areas having large areas. This situation creates undesirable hot-spots-- that is, regions of the nanowire that are more sensitive to external charge than others. Another disadvantage of the line edge roughness is that the sensor response measurement is not as accurate (in an absolute scale) nor consistent from nanowire to nanowire because LER is random and not repeatable.

In this work, the root cause of LER is traced to the use of a Chromium (Cr) hard mask to form the nanowire sensor in the state of the art fabrication process [25]. The lift off patterning process used to form this hard mask results in shearing/tearing of the chromium and results in rough edges in the Cr mask. This roughness is then transferred to the silicon nanowire in a subsequent etch.

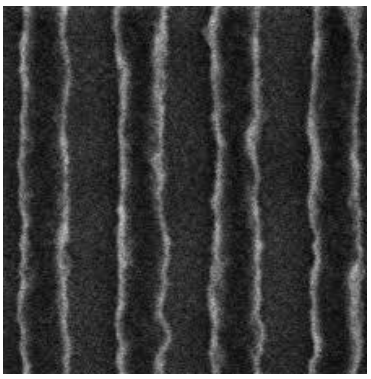

Figure 4.1 Scanning electron microscope image showing Line edge roughness (LER). Node spacing is 65 nm [43]

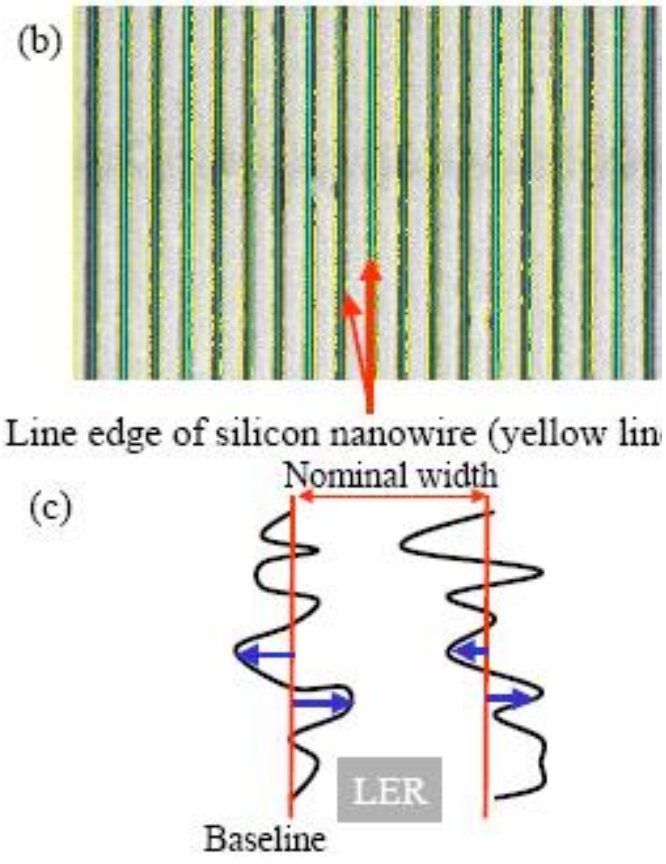

Figure 4.2 Array of fabricated silicon nanowires showing line edge roughness, measured in a CD-SEM. [44]

This presents two compelling reasons to eliminate chromium from the nanowire

formation process, but an alternate mask/etch process is needed to replace the chromium liftoff hardmask etch process.

4.1.2 Sensor Drift Over Time

When making a pH measurement, consistent nanowire response over time is important. Any time-varying response of the sensor not due to changes in the pH is referred to as sensor drift over time. A principal cause of sensor drift has been traced to ions and charges adhering to the dielectric surface and remaining adhered after the fluid pH has been altered. PECVD films are known to have a higher pinhole density than LPCVD films, which is a leading cause of sensor drift [42].

This work makes the case for a totally new process for forming the nanowires. From the discussion above, two major changes to the process would improve three aspects of the nanowire. Removing chromium as the hardmask and replacing PECVD nitride with LPCVD nitride would improve sensor yield, consistency, and output drift.

4.2 Novel Fabrication Improvements

Using a top down fabrication method with electron beam lithography and optical lithography, SiNW can achieve small dimensions (50 nm wide), high reproducibility and reliability. Silicon on insulator (SOI) wafers are used to fabricate the nanowire sensors. SOI wafers are fabricated with a thin monocrystalline silicon layer bonded on top of an insulator having very low defect density. Previous researchers such as Park and Choi use a top down fabrication method as outlined in chapter 1.

4.2.1 Silicon Oxide Hard Mask

One of the challenges in this work is to achieve the fabrication of small and large features using a single etch mask. Small features can be patterned using Electron beam lithography, however, the write time is directly proportional to the area on the wafer being written (exposed). This limitation does not exist in optical (visible light) lithography because the exposure is a flood exposure, but optical lithography has a limitation of diffraction limited feature size resolution. These disparate size requirements are overcome by using a combination of electron beam lithography and optical lithography integrated into one etch step. The electron beam is used to form the small features (nanowire sensors) and the optical lithography is used to form the large features (leads and pads). In this way, the e-beam write time is short, used only as needed for high resolution, while necessarily large features are pattered more crudely by optical lithography, yet they are etched in the same step. Since the optically-sensitive film used is different for optical and e-beam exposures, the patterns must be combined in a separate masking layer under the film before being transferred to the silicon to form the nanowire. As described previously, a pattern can be transferred by liftoff of a hard mask material such as chromium. In the state of the art fabrication process a lift off process is employed such that the nanowires can be formed by deposition of metal (chromium) mask followed by lift off. This process is repeated twice, once for the large features using optical lithography, and again for small nanowire features using e-beam lithography. The advantage of this method is that the masking layers are additive. That is, the chromium is added where a feature was written by the patterning process. This process could be repeated as many times as desired to form a composite image. In Boolean terms, the final pattern, P, is P = A + B + C_+ D … The chromium may be thicker where there is overlap, but this is of little consequence for a hardmask.

A better approach used in the present work is to use a silicon oxide hard mask to form the nanowire sensors. For instance, a silicon oxide (SiO2) is thermally grown on top of the Silicon as a sacrificial hardmask layer. Once the nanowires are exposed with an e-beam pattern and developed, then this pattern is transferred to the oxide layer using an oxide etch. Subsequently, optical lithography is used to pattern large features (wires, bondpads), while grossly protecting the previously etched nanowire region. This pattern is transferred to the oxide hardmask as well. After removing the photoresist, the silicon is

etched using the oxide as a hardmask, and both large and small features are formed simultaneously in the silicon (SOI) layer.

This change is not a simple substitution of oxide for chromium in the process, for several reasons. The main difference is that, unlike the chromium mask process, the oxide mask is deposited before any patterning. Therefore, the process is subtractive. This requires different photomasks/patterns, and not just a simple reversal of patterns. The final pattern, P, will be P = ALL – A – B – C …. Where ALL is the entire wafer. This means that the nanowire must be carved from the area outside to leave the small wire. A novel process and pattern are used. After the oxide is thermally grown, E-beam lithography is used to make two trenches on either side of what will become the nanowire. These trenches are spaced apart by the desired nanowire width. The width of the trenches themselves are not critical, but must be wide enough that they can be resolved within the subsequent optical lithography step, for example, 2 micron. This represents a larger write time than simply writing the nanowire, but is still manageable. Write times per nanowire were on the order of 60 seconds. Most of the time per nanowire is spent in setup, for instance, aligning the beam, focusing, etc, so the actual beam scan time is not critical for an area of a few hundred micron squared. Following the e-beam patterning, an oxide etch is performed on the trenches.

Next the optical pattern is performed. The e-beam resist is first removed, followed by a standard optical lithography process. The mask design is critical, mainly because of the overlap regions. The optical resist must protect the bondpad and lead wire areas, but also must protect the previously e-beam patterned nanowire area with a micron-sized protection zone. The trenches provide tolerance for the optical lithography step. So long as the edges of the optical mask register in the e-beam formed trenches, the pattern is sufficiently registered. The oxide hardmask is again etched to form the bondpads and lead wires. The oxide hardmask now comprises the nanowire (edges formed via e-beam) and the large features. After removal of the optical photoresist, a silicon etch step is now be used to form the silicon nanowire and bondpads in one etch step. The sacrificial oxide hardmask is then wet stripped.

Straight side walls are achieved using a silicon etch, with oxide mask, using a Cl/HBr plasma etch process which has a selectivity of approximately 10 to 1 with oxide. This dramatically reduces the poor line edge roughness (LER). One additional advantage of this approach is that, in the absence of chromium, this process becomes truly CMOS compatible, and therefore a high temperature process can be used for forming the critical dielectric over the nanowire.

4.2.2 High Temperature Dielectric

Another contribution in this work is the improvement of pin hole density in the dielectric. After forming the nanowire, a dielectric film is deposited around the wire, encapsulating it and electrically insulating it from the surrounding fluid. This prevents charge recombination at the wire-solution interface. This dielectric is necessarily very thin (a few nm) so that the electric field penetrates from the solution into the nanowire, causing charge depletion. Plasma Enhanced Chemical Vapor Deposition (PECVD) used in the state of the art fabrication process for depositing the dielectric film generally produces a film with higher pin hole density when compared to other deposition methods such as Low Pressure Chemical Vapor Deposition.

In this work, Low Pressure Chemical Vapor Deposition (LPCVD) is used, which is performed at higher temperatures (~800C). A synergistic result of the redesigned process in this work is that by eliminating the Cr hardmask (which was done principally to improve LER) the process remains CMOS-compatible at this point. This allows high temperature processing, and thus, the use of LPCVD nitride or thermal oxide as the dielectric material reducing the amount of pin holes and subsequently reducing sensor drift over time which remains a challenge in devices. By making the process CMOS compatible, many industry standard options are available for high performance dielectrics. A composite thermal oxide followed by thin LPCVD nitride is possible, as is common in critical tunneling dielectrics of nonvolatile memory (EEPROM or flash memory) devices.

4.2.3 Parasitic Resistances

Large features such as leads and pads contribute a significant amount of parasitic resistance. This parasitic resistance is undesirable because it adds to the overall resistance of the sensor without increasing the change in resistance due to charge. This decreases the ability of the nanowire to sense small charge concentrations because the percentage change is smaller. In the state of the art process, the entire device layer is doped to the

same concentration as the nanowire, in one blanket ion implant step. The doping in the nanowire is varied by design from sensor to sensor for dynamic range advantages, but the leads and pads should be as low resistance as possible (heavy doping)

A way to minimize this undesirable resistance is by heavily doping the areas where the leads and pads are formed. This requires an additional implant step which can be done at the wafer level as shown in the novel fabrication process table. By increasing the conductivity of the leads and pads, parasitic resistance can be reduce allowing a more accurate measurement of the nanowire. The metal forming the contacts is allowed to contact the leads as well as the pads, further reducing the parasitic resistance. Another benefit to heavy doping is the Schottky barrier between the metal and the semiconductor is greatly reduced [38]. This helps with sensor sensitivity since the majority of the resistance is now in the nanowire rather than parasitics.

4.2.4 Detailed Novel Fabrication Process

A novel fabrication process is used to improve on these three challenges mentioned above. Using SOI (Silicon on insulator) wafer, a thin thermal oxide (30 nm) is grown as the sacrificial hardmask layer. A further improvement in the process is that it can be made wafer-scale, saving development time for rapid short-loop development. Thus, alignment marks are placed at the wafer level using optical lithography. This allows to ion implant boron for reduce parasitic resistances. Once the wafer is diced, e-beam lithography is used to form the nanowire sensor (small features) shape into the silicon oxide hard mask. Optical lithography is then employed to form the leads and pads (large features) shape using photoresist as a mask and this shape is transferred into the silicon oxide with an etch (while grossly protecting the nanowire region). Once both large and small features are formed in the oxide hardmask, the aggregate pattern is etched into the SOI layer, forming the nanowire and all associated leads and pads. A layer of silicon nitride dielectric is deposited as passivation layer. Silicon nitride is used as an ion blocking electrical insulator. Holes are etched in the nitride on the pads, and finally bondpad contact metal is deposited followed by liftoff.

]

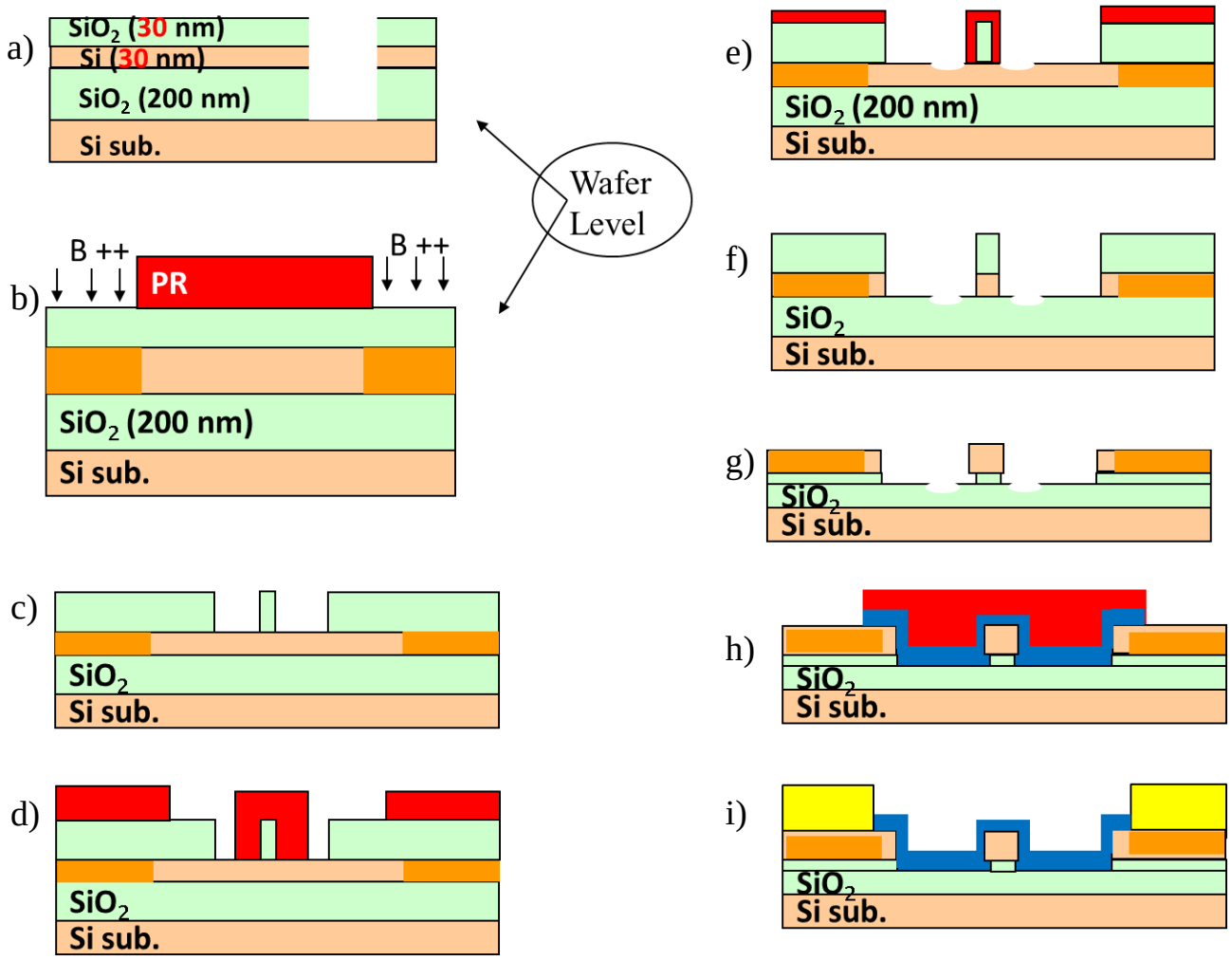

Figure 4.3 Description of the novel fabrication process. Step a) alignment marks and b) heavy ion doping to reduce parasitic resistance can be done at the wafer level. Step c) is the oxide mask etched after writing the nanowire sensor with the e-bem, the nanowire sensor is in the center. Step d) shows the nanowire sensor protected with photoresist and the large features have been drawn using optical lithography. Step e) and f) are two etches to form the nanowire and the large features. Step h) is the dielectric over the nanowire sensor and finally step i) is metal deposition and lift-off.

4.2.5 Fabrication Results of Silicon Nanostructures

Silicon nanowires were fabricated using the novel fabrication process described in previous section. The metal contact used in this fabrication process was titanium and gold (Ti/Au) and successful liftoff was achieved.

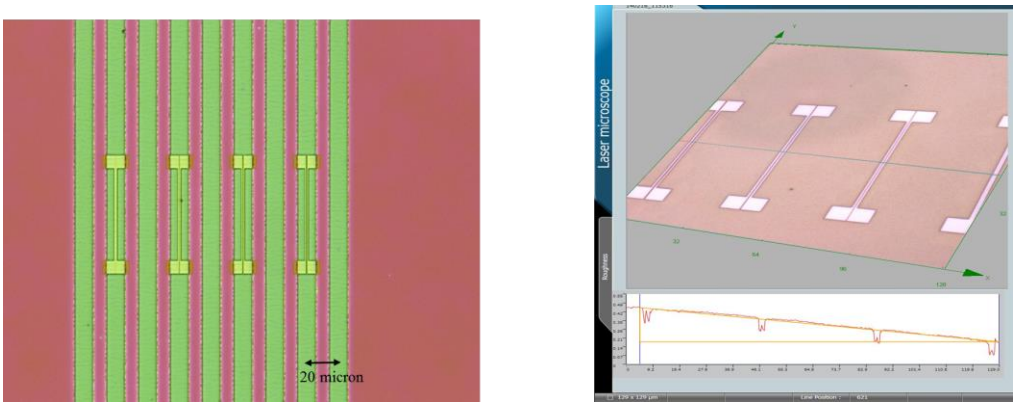

Figure 4.4. The picture on the left shows an array of silicon nanowires. Alignment between the e-beam and the optical lithography is well achieved. The picture on the right shows another array of silicon nanowires after etching the oxide (only 30 nm) and stopping on silicon.

After the fabrication was completed, the devices were tested in buffer solution using pH 4, 7 and 10. These tests were conducted in the dark to reduce noise interference. Experimental data was obtain as shown in Figure 4.5

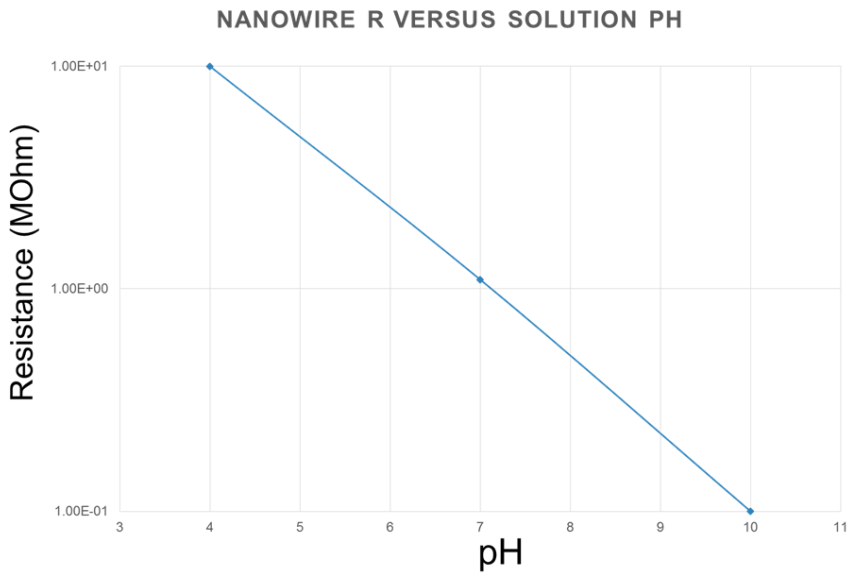

Figure 4.5 showing experimental results of the fabricated devices. The Resistance versus pH graph shows a linear relation as expected from the analysis.

4.3 Cell/System Fabrication

The main added feature of the dynamic measurement cell are the outer electrodes. These electrodes are necessarily tall (approximately 2 microns in height) in order to maintain a constant electric field and maintain an optimum starting ionic collimated charge profile. These tall features are difficult to fabricate in an integrated process alongside the nanowire sensors which are very small in the height direction (approximately 50 nm) Therefore, a separate substrate is used to fabricate these outer electrodes, and the two substrates are subsequently bonded together. One advantage is that the outer electrodes can be fabricated using standard semiconductor fabrication techniques. Starting with a silicon wafer, conductive (heavily doped) polysilicon is desposited, then deep reactive ion etched to form the fluid channel. Since the outer electrodes are conductive and in contact with the fluid, a thin silicon oxide is necessary to protect the walls and prevent electrochemical reactions. The thickness of this oxide is not critical. 100nm is sufficiently thick to prevent charge transfer, and does not significantly change the electric field in the fluid channel when voltage is applied.

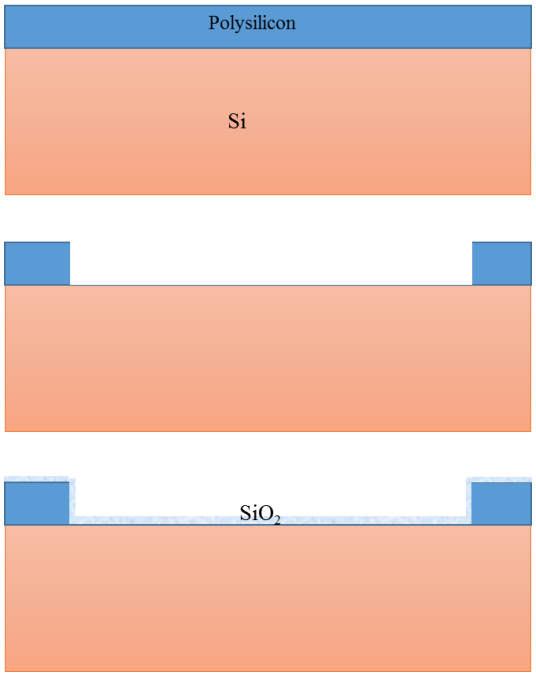

Figure 4.6 describes the fabrication process for the outer electrodes. Outer electrodes are fabricated on a different substrate and later integrated with the nanowire sensor device.

CHAPTER 5. CONCLUSIONS AND FUTURE WORK

Many industries such as pharmaceutical, pollution control, etc require careful, accurate measurement of pH. Particularly, in the medical field, doctors would like to monitor blood pH during a surgical procedure, but current methods are slow, inaccurate and require pre-processing of the blood. The silicon nanowire system presented in this work can achieve measurement of true pH in situ, in real time, using unprepared raw blood. This silicon nanowire system can measure true pH which is the negative log of the hydrogen ion activity in the presence of other interfering ions such as sodium and potassium. To achieve this goal careful design of the system is necessary as well as a method for operating the same.

The system is composed of outer electrodes (tall walls) with a fluidic channel in between them. This fluidic channel can be designed with different widths depending on the type of fluid and the species of interest that wish to be measured. Some of the examples shown in this work consider a channel 20 μm wide. The silicon nanowires are located in between these two outer electrodes. Placement of the nanowire sensor in the channel is important in order to sense the desired species of interest. Silicon nanowires are small so an array of nanowires can be fabricated to allow more dynamic range and they are CMOS compatible so they can easily be integrated with other electronics.

Various modes of operation have been developed in this work that allow the species to separate as they cross the channel and therefore allowing measurement of various species. One particular mode of interest is the Time of Flight mode of operation which consists on placing a potential difference between the outer electrodes that generates an external electric field. The ions in the fluid respond to this electric field such that the negative ions migrate to one side and the positive ions migrated toward the opposite side depleting the fluid of any mobile charge. When the field is reversed, the ions begin to travel by drift-diffusion methods toward the opposite electrode. Since each specie of ions has a particular mobility, the ions naturally travel with different velocities and the groups of each species begin to form or separate. The ions arrive at the nanowire in microseconds, making, for the first time, a dynamic measurement. This measurement is orders of magnitude faster than regular methods currently used by industrial team members who rely on paper strips or glass electrode

type methods.

The modeling performed in this work is consistent with the theoretical analysis, showing a good match with the displacement of the species as they travel with time and it is also consistent with the diffusion length which determines how sharp the peak of the Gaussian is. This is important because a small diffusion length means that diffusion is less significant and enables the nanowire sensor to sense the total concentration of that particular species.

This silicon nanowires are fabricated using a novel top down fabrication method which is truly CMOS compatible. It differs from the state of the art fabrication process by eliminating the use of the double chromium deposition and lift off used to form the small and large features. Instead, silicon oxide is used as a hardmask and both ebeam and optical lithography are used to form the small and large features to reduce ebeam writing time. In addition, to form the dielectric (silicon nitride) film, Vapor Deposition (LPCVD) is used instead of Plasma Enhanced (PECVD) to reduce pin hole density and improve on sensor drift over time. Experimental results show a linear relation between pH and change in electrical resistance of the nanowire which is consistent with previous results performed by other researchers.

In summary, a novel sensor has been developed using a new fabrication process which improves the state of the art fabrication process by reducing pin-hole density, line edge roughness and sensor drift overtime. In addition, the development of new methods for driving the nanowire sensor using electrospectroscopy allows selective ion screening benefits which include ion species identification, measurement of true pH, high sensor sensitivity by optimizing a new driving mechanism and functionalization of the nanowire sensor for bio-detection. Noise reduction is still a challenge when making measurements which needs to be addressed in future work. Modeling of various modes of operation can provide significant information useful to design a nanowire sensor system that is optimum for the desired species identification. Further analysis on dynamic range and blocking of the x component of the electric field can also be explored in future work. More fabrication and experimental testing using other modes of operation could be useful to study and compared to the modeling and theoretical analysis and can also be addressed in future work. Dynamic range is also widely explored and fabrication of both retrograde doping profile nanowires and n-type nanowires could also be studied in future work.

REFERENCES

[1] H. Galster, “pH Measurement: Fundamentals, Methods, Applications, Instrumentation”, Wiley-VCH, 1991.

[2] W. Lyons, G. Plisga “Standard Handbook of Petroleum and Natural Gas Engineering”, Golf Professional Publishing, 2011.

[3] D. Harris, “Quantitative Chemical Analysis”, Macmillan, 2010.

[4] C. Westcott, “pH Measurements”, Elsevier, 2012.

[5] G. McMillan, R. Cameron, “Advanced pH Measurement and Control”, ISA, 2005.

[6] T. Sakurai, Y. Husimi, “Real Time Monitoring of DNA polymerase reactions by a micro ISFET pH sensor”, Anal. Chem, 64 (17), pp 1996-1997, 1992.

[7] I. Park, Z. Li, A. Pisano, R. S. Williams, “Top Down Fabricated Silicon Nanowire Sensors for Real-time Chemical Detection”, Nanotechnology, V.21, number 1, 2009.

[8] F. Patolsky, G. Zheng, C. Lieber, “Fabrication of Silicon Nanowire devices for ultrasensitive, label-free, real-time detection of biological and chemical species”, Nature Protocols 1, 1711-1724, 2006.

[9] J. Dahl, “Ion Mobility and Mass Spectrometry”, Makinions, 2014.

[10] H. Hillbert, S. Greg, “Capabilities and Limitations of Ion Mobility Spectrometry for Field Screening Applications”, Technology Review, Field analytical chemistry and technology, (3), pp 119-134, 1997.

[11] J. Sauer, B. Zeghbroeck “Field effect transistor device for ultra fast nucleic acid sequencing”, Patent EP 2278317, 2011.

[12] V. Kumar, “Nanosilicon”, Elsevier, 2011.

[13] J.L. Coffer, “Semiconducting silicon nanowires for biomedical applications”, Elsevier, 2014.

[14] Y. Omura, “Advanced semiconductor on insulator technology and related physics 15”, The Electrochemical Society, 2011.

[15] C. Enz, A. Kaiser “MEMS-based circuits and systems for wireless communication”, Springer Science and Business Media, 2012.

[16] R. Hobbs, N. Petkov, J. Holmes, “Semiconductor Nanowire Fabrication by Bottom

up and Top-Down Paradigms", Chem. Mater, 24 (11), 1975-1999, 2012.

[17] G. McMillan, R. Cameron, "Advanced pH Measurement and Control", ISA, 2005.

[18] T. Sakurai, Y. Husimi, "Real Time Monitoring of DNA polymerase reactions by a micro ISFET pH sensor", Anal. Chem, 64 (17), pp 1996-1997, 1992.

[19] E. L. Cussler, "Diffusion: Mass Transfer in Fluid Systems", Cambridge University Press, 2009.

[20] W. Lyons, G. Plisga "Bottom up Fabrication process", Golf Professional Publishing, 2011.

[21] F. Zorgiebel, S. Pregl, L Romhildt, J Opitz, "Schottky barrier-based silicon nanowire pH sensor with live sensitive control", Nanoresearch, Vol 7, Issue 2, 2014.

[22] Z. Li, Y. Chen, X. Li, T. I. Kamins, "Sequence Specific Label Free DNA Sensors Based on Silicon Nanowires", Nanoletters, 4 (2), 245-247, 2004.

[23] E. Stern, J. Kelmic, D Routenberd, P. Wyremback, "Label-free immunodetection with CMOS-compatible semiconducting nanowires", Nature 445, 519-522, 2007.

[24] H. Tong, S. Chen, W. van del Wiel, "Novel Top-Down Wafer-Scale Fabrication of Single Crystal Silicon Nanowires", NanoLetters, 9 (3), 1015-1022, 2009.

[25] I. Park, Z. Xuema, A. Pisano, R. Williams, "Towards the silicon nanowire-based sensor for intracellular biochemical detection", Biosensors and Bioelectronics, 22, Elsevier, 2007.

[26] Y. Chen, X. Wang, S. Erramilli, "Silicon-based nanoelectronic field-effect pH sensor local gate control", Applied physics letters, 89, 2006.

[27] R. Elsair, "Fundamentals of Chemistry", Romain Elsair and Ventus Publishing, 2012.

[28] Y. Jin, "Electromagnetic Scattering Modelling for Quantitative Remote Sensing", World Scientific, 1993.

[29] E. Weisstein, "CRC Encyclopedia of Mathematics", CRC Press, 2002.

[30] B. Bhushan, "Springer Handbook of Nanotechnology", Springer Science & Business Media, 2010.

[31] B. Kirby, "Micro-and Nanoscale Fluid Mechanics: Transport and Microfluidic Devices", Cambridge University Press, 2010.

[32] T. Zohdi, P. Wriggers, "An Introduction to Computational Micromechanics",

Springer-Verlag Berlin Heidelberg, 2005.

[33] T. Zohdi, "Dynamics of Charged Particle Systems Modeling, Theory and Computation", SpringerBriefs in Applied Science and Technology, 2012.

[34] D. Griffiths, "Introduction to Electrodynamics", Pearson, 2015.

[35] A. Schwab, "Field Theory Concepts: Electromagnetic Fields, Maxwell's Equations, Grad, Curl, Div, Etc…", Springer-Verlag, 1st Edition, 1988.

[36] N. Giordano, "College Physics", Cengage Learning, 2012.

[37] S. Sze, K. Ng, "Physics of Semiconductor Devices", Wiley, 2006.

[38] S. Wolf, "Silicon Processing for the VLSI, Vol 3: The Submicron MOSFET", Lattice Press, 1994.

[39] H.K. Versteeg, W. Malalasekara "Introduction to Computational Fluid Dynamics: The Finite Volume Method", Longman Group, 1995.

[40] S. Wolf, "Silicon Processing for the VLSI, Vol 1: Process Technology", Lattice Press, 1996.

[41] S. Wolf, "Silicon Processing for the VLSI, Vol 4: Deep Submicron Process Technology ", Lattice Press, 2002.

[42] L. Ru-Shi, "Controlled Nanofabrication: Advances and Applications", CRC Press, 2012.

[43] A. Yamaguchi, R. Nakagaki, "CD SEM Technologies for 65 nm Process Node", Hitachi Revies, vol 54, No 1, 2005.

[44] I. Park, "Nanowire Sensor for Real-time Chemical and Biological Detection", University of California Berkeley, 2007.